



Universiteit  
Leiden  
The Netherlands

## Shining light on polymeric drug nanocarriers with fluorescence correlation spectroscopy

Schmitt, S.; Nuhn, L.; Barz, M.; Butt, H.J.; Koynov, K.

### Citation

Schmitt, S., Nuhn, L., Barz, M., Butt, H. J., & Koynov, K. (2022). Shining light on polymeric drug nanocarriers with fluorescence correlation spectroscopy. *Macromolecular Rapid Communications*, 43(12), 2100892. doi:10.1002/marc.202100892

Version: Publisher's Version

License: [Creative Commons CC BY 4.0 license](https://creativecommons.org/licenses/by/4.0/)

Downloaded from: <https://hdl.handle.net/1887/3281254>

**Note:** To cite this publication please use the final published version (if applicable).

# Shining Light on Polymeric Drug Nanocarriers with Fluorescence Correlation Spectroscopy

Sascha Schmitt, Lutz Nuhn, Matthias Barz, Hans-Jürgen Butt, and Kaloian Koynov\*

The use of nanoparticles as carriers is an extremely promising way for administration of therapeutic agents, such as drug molecules, proteins, and nucleic acids. Such nanocarriers (NCs) can increase the solubility of hydrophobic compounds, protect their cargo from the environment, and if properly functionalized, deliver it to specific target cells and tissues. Polymer-based NCs are especially promising, because they offer high degree of versatility and tunability. However, in order to get a full advantage of this therapeutic approach and develop efficient delivery systems, a careful characterization of the NCs is needed. This review highlights the fluorescence correlation spectroscopy (FCS) technique as a powerful and versatile tool for NCs characterization at all stages of the drug delivery process. In particular, FCS can monitor and quantify the size of the NCs and the drug loading efficiency after preparation, the NCs stability and possible interactions with, e.g., plasma proteins in the blood stream and the kinetic of drug release in the cytoplasm of the target cells.

moderate number of nanocarriers have entered clinical trials and just a few became first line therapies.<sup>[8]</sup>

One of the major challenges in the development of efficient drug NC-based therapies is the need for precise monitoring of the NCs characteristics such as size, surface functionalization, drug loading, and stability. Such monitoring is essential over the entire delivery process: from the preparation of the NCs, through their circulation in the blood system, until the drug release in the target cells or tissues. For example, it is important to control that the NCs do not aggregate, degrade or prematurely release their cargo already during their shelf life. These unfavorable processes can become even more likely once the NCs are injected in the blood system of a patient or an animal model, where they face an environment with high concentration of cells,

proteins and other solutes. Finally, it is important to monitor and quantify the cargo release in the target cells and even follow the fate of the delivered therapeutic agents into a specific cell compartment. Thus, the NCs have to be characterized in several different environments with increasing complexity. These include i) aqueous buffer conditions for the preparation and storage, ii) blood plasma and whole blood that are the relevant media while NCs circulate in the blood system, and iii) the cytosol of the target cells during the final, drug release step.


It is clear that a combination of complementary experimental methods has to be used in order to obtain a comprehensive understanding on the fate of the NCs during the whole delivery process. While a broad range of such methods for NCs characterization have been discussed in recent reviews,<sup>[9,10]</sup> in this

## 1. Introduction

Since Ringsdorf's concept of pharmacologically active polymers for improved drug delivery,<sup>[1]</sup> various types of polymer-based nanocarriers (NCs) have been developed to enhance the performance of small drug molecules, proteins or nucleic acids clinics.<sup>[2]</sup> They can alter their pharmacokinetics by, e.g., protection from the environment during the transport through the blood system, focused delivery to a target site-of-action and reduction of potential side effects.<sup>[3]</sup> Over the last four decades, NC-based drug delivery approaches have been applied in various fields ranging from cancer treatment<sup>[4–6]</sup> to antiviral vaccine development,<sup>[7]</sup> yet, despite large research efforts only a

S. Schmitt, L. Nuhn, H.-J. Butt, K. Koynov  
 Max Planck Institute for Polymer Research  
 Ackermannweg 10, Mainz 55128, Germany  
 E-mail: koynov@mpip-mainz.mpg.de

M. Barz  
 Leiden Academic Centre for Drug Research (LACDR)  
 Leiden University  
 Einsteinweg 55, Leiden 2333 CC, The Netherlands

 The ORCID identification number(s) for the author(s) of this article can be found under <https://doi.org/10.1002/marc.202100892>

© 2022 The Authors. Macromolecular Rapid Communications published by Wiley-VCH GmbH. This is an open access article under the terms of the Creative Commons Attribution License, which permits use, distribution and reproduction in any medium, provided the original work is properly cited.

DOI: 10.1002/marc.202100892

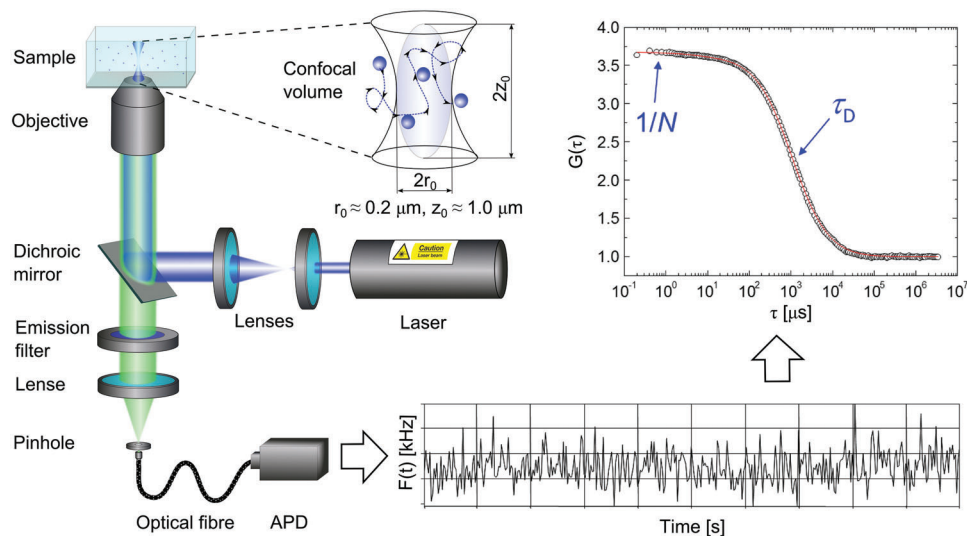


**Figure 1.** Schematic representation of a typical confocal FCS setup and its principle of operation. Reproduced with permission.<sup>[23]</sup> Copyright 2012, Elsevier.

review we focus on the fluorescence correlation spectroscopy technique, which can assist to provide a deeper insight, especially in a complex biological environment. We show that due to its single molecule sensitivity, selectivity, and very small ( $<1 \mu\text{m}^3$ ) probing volume, FCS can serve as a powerful and versatile tool for the characterization of fluorescently labeled polymeric NCs at all stages of the delivery process and provide information on size, surface functionalization, drug loading efficiency, interactions with plasma proteins or other species as well as on triggered or premature decomposition and/or cargo release.

## 2. Basic Principles of Fluorescence Correlation Spectroscopy

Fluorescence correlation spectroscopy (FCS) technique is commonly applied to study small (1–500 nm) fluorescence species dispersed in fluid environments. FCS measures the diffusion coefficient and hydrodynamic radius of the species, their concentration, and fluorescent brightness. The technique was introduced in the early 1970s,<sup>[11–13]</sup> but gained more attention in the 1990s, when it was combined with confocal microscopy<sup>[14–16]</sup> that enabled single-molecule detection sensitivity. Since then FCS has become a powerful tool in various research fields ranging from molecular and cell biology to polymer, colloid, and interface science.<sup>[17–26]</sup> Nowadays, most commercial confocal microscopes have the option for performing FCS studies.

The setup for FCS experiments is basically identical to that of a confocal microscope (Figure 1). Briefly, a laser beam is expanded, reflected by a dichroic mirror and focused into the studied sample using a high numerical aperture microscope objective. The excited fluorescence light is collected by the same objective and after passing through the dichroic mirror, an emission filter and a confocal pinhole, it is directed to a fast and sensitive detector, typically an avalanche photo diode or photomultiplier operating in single photon counting mode. These settings result in the formation of a very small ( $<1 \mu\text{m}^3$ ) confocal observation volume  $V_{\text{obs}}$  in the studied sample (Figure 1). Only fluorescence light

originating from fluorophores in this volume can be detected. In confocal microscopy imaging, the confocal volume is scanned through a sample to detect the position of immobilized fluorescence species. By contrast, during an FCS experiment the confocal volume is kept in a fixed place and the Brownian diffusion of the studied fluorescent species through this volume is recorded. As the species enter and leave the confocal observation volume they create temporal fluctuations in the detected fluorescence intensity,  $F(t)$ , that are recorded and analyzed by an autocorrelation function

$$G(\tau) = 1 + \frac{\langle \delta F(t) \delta F(t + \tau) \rangle}{\langle F(t) \rangle^2} \quad (1)$$

Here  $\delta F(t) = F(t) - \langle F(t) \rangle$  and  $\langle \rangle$  denotes time average. A typical experimentally measured autocorrelation function is shown in Figure 1. It has a characteristic decay time  $\tau_D$  (called diffusion time) reflecting the average time, which the studied fluorescence species needs to diffuse through the confocal observation volume.

It has been shown theoretically that for an ensemble of  $m$  different types of freely diffusing fluorescence species,  $G(\tau)$  has the following analytical form<sup>[17]</sup>

$$G(\tau) = 1 + \left[ 1 + \frac{f_T}{1 - f_T} e^{-\tau/\tau_T} \right] \frac{1}{N} \sum_{i=1}^m \frac{f_i}{\left[ 1 + \frac{\tau}{\tau_{D_i}} \right] \sqrt{1 + \frac{\tau^2}{S^2 \tau_{D_i}^2}}} \quad (2)$$

Here,  $N$  is the average number of diffusing fluorescence species in the observation volume,  $f_T$  and  $\tau_T$  are the fraction and the decay time of the triplet state,  $\tau_{D_i}$  is the diffusion time of the  $i$ th species,  $f_i$  is the fraction of component  $i$ . The diffusion time,  $\tau_{D_i}$ , is related to the respective diffusion coefficient,  $D_i$ , through  $\tau_{D_i} = r_0^2/4D_i$ . The so-called structure parameter  $S = z_0/r_0$ , is defined as the ratio of axial to radial dimensions of  $V_{\text{obs}}$ . Usually, the width of  $V_{\text{obs}}$  is 300–500 nm, its height 1.5–2  $\mu\text{m}$  and thus  $S \approx 5$ . In a typical FCS experiment the measured

autocorrelation function (Equation (1)) is fitted with the analytical expression (Equation (2)). In this way one obtains the diffusion times and thus the diffusion coefficients of the fluorescent species, their concentration ( $N/V_{\text{obs}}$ ) and molecular (or particle) fluorescence brightness ( $\langle F(t) \rangle / N$ ). Furthermore, the hydrodynamic radii of the species can be calculated from their diffusion coefficients using the Stokes–Einstein (SE) relation

$$R_{\text{H}} = \frac{k_{\text{B}} T}{6\pi\eta D} \quad (3)$$

Here,  $k_{\text{B}}$  is Boltzmann's constant,  $T$  is the temperature, and  $\eta$  is the viscosity of the solution. It should be emphasized at this point that both the SE relation (Equation (3)) and the viscosity term that it includes depend on temperature. Even more importantly, the behavior of various nanocarrier systems and biological fluids discussed below may have strong temperature dependence. That is why temperature control during an FCS experiment is essential for proper data evaluation.

### 3. FCS Characterization of NCs in Aqueous Buffer Solutions

#### 3.1. Measuring NCs Size and Drug Loading Efficiency

Probably the simplest, but also most commonly used application of the FCS technique in NC-based drug delivery studies is to measure the hydrodynamic radii of NCs and therapeutic compounds. In this respect, FCS is quite similar to the commonly used dynamic light scattering (DLS) technique, with one major difference: FCS is based on fluorescence detection. Thus, to enable FCS, one should use either the intrinsic fluorescence of the studied species, e.g., for drugs like doxorubicin,<sup>[27,28]</sup> or label the NCs or the therapeutic agents with fluorescent dyes. This is a relatively simple task, because fluorescent labeling protocols are well established nowadays and wide range of fluorescently labeled polymers, antibodies or RNA molecules are commercially available. Moreover, in many studies the NCs and their cargo must be fluorescently labeled anyway for confocal laser scanning microscopy or optical whole animal imaging.

On the other hand, it is the fluorescence-based detection that enables the unique single molecule sensitivity and selectivity of the FCS technique. Due to its sensitivity, FCS can be applied to study species with diameters from roughly 500 nm to less than 1 nm at concentrations down to sub-nanomolar in sample volumes of less than 20  $\mu\text{L}$ . Due to its selectivity, FCS detects only the fluorescent species, even if larger, but nonfluorescent species are present in the studied solution. This makes the FCS technique particularly suited to monitor and quantify the loading of fluorescent therapeutic molecules in polymeric NCs.

As an example, **Figure 2** shows the results of FCS investigations of the encapsulations of Atto590-labeled siRNA into cationic nanohydrogel particles.<sup>[29]</sup> First, a solution containing only labeled siRNA was studied. The measured autocorrelation curve (red) was fitted with Equation (2) ( $m = 1$ ) yielding a diffusion time of 130  $\mu\text{s}$  that corresponds to a hydrodynamic radius of  $\approx 2.3$  nm for this double-stranded oligonucleotide. However, upon mixing the siRNA with the cationic nanohydrogel particles at a weight-to-weight ratio of 80:1 NP/siRNA, the autocorrelation curve (blue)

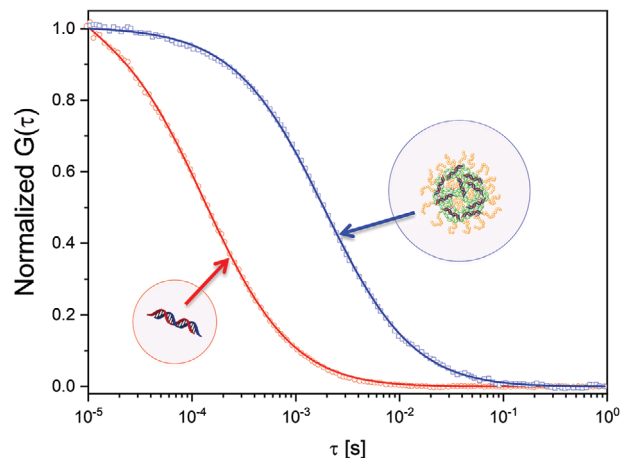


**Figure 2.** FCS autocorrelation curve of Atto590-labeled siRNA alone (red symbols) and in the presence of cationic nanohydrogel particles (blue symbols). The solid lines represent the corresponding single component fits (Equation (2),  $m = 1$ ). Adapted with permission.<sup>[29]</sup> Copyright 2012, American Chemical Society.

shifted significantly to higher decay times (Figure 2) indicating that siRNA molecules are now not diffusing freely, but are associated with the much larger and thus slowly diffusing nanohydrogel particles. The measured autocorrelation curve (blue) was fitted with Equation (2) ( $m = 1$ ) yielding a diffusion time of 1900  $\mu\text{s}$  and thus an average hydrodynamic radius of about 33 nm for the siRNA loaded nanohydrogel particles. These results clearly confirmed that the siRNA molecules were loaded in the nanocarriers. It is important to note that the loading cannot be investigated in a similar manner with a nonselective method like, e.g., DLS, because it monitors all species present in the solution (fluorescent or nonfluorescent) based only on their size and thus cannot distinguish between loaded and empty NCs.

FCS can also be used to measure the NCs loading efficiency, based on the so-called molecular (or particle) fluorescence brightness of the studied species. This parameter estimates how strong the fluorescence signal is that originates from an individual fluorescent molecule (or particle) under certain FCS experimental conditions. It is defined as  $\langle F(t) \rangle / N$ , where  $\langle F(t) \rangle$  is the average intensity of the detected fluorescence signal and  $N$  is the average number of molecules in the confocal observation volume (see Section 2 for details). Thus, the loading efficiency per particle can be evaluated by dividing the NC fluorescence brightness by the fluorescence brightness of an individual cargo molecule. For example, in the system discussed in Figure 2 the FCS experiments performed in solutions containing only the labeled siRNA yielded a value of 9 kHz per molecule for the fluorescent brightness of an individual siRNA molecule. The fluorescent brightness of the siRNA-loaded nanohydrogel particles was 370 kHz per particle. Thus, dividing 370 by 9 the authors estimated an average loading efficiency of  $\approx 40$  siRNA per nanocarrier. It should be noted that the loading efficiency measured in this way can be partially underestimated due to possible fluorescence quenching, especially at very high loadings, at which the fluorophores can be densely packed. One simple way to overcome such quenching effects is to combine fluorescently labeled siRNA with nonlabeled ones in a well-defined ratio (e.g., 1 to 10) and therefore decrease

the overall density of the fluorophores. It can then be applied to recalculate the real drug load by multiplying it with the respective dilution factor (e.g., 10). This approach can also be used for evaluating the loading efficiency for other types of fluorescently labeled therapeutic substances.

One of the first reports on applying FCS to investigate loading of therapeutic molecules in nanocarriers was published in 2001 by Delie et al.<sup>[30]</sup> who studied the loading of rhodamine 6G-labeled 19mer oligonucleotides on preformed cationic monomethylaminoethylmethacrylate nanoparticles. In a follow up study,<sup>[31]</sup> the loading of oligonucleotides on cationic polybutylcyanoacrylat nanoparticles was addressed. In 2006, Rigler and Meier<sup>[32]</sup> studied the encapsulation of small dye molecules and fluorescently labeled Avidin in nanocontainers prepared from amphiphilic triblock copolymers and introduced the described above method to evaluate the drug loading efficiency using molecular/particle fluorescence brightness. In the last two decades, FCS has become a powerful tool to quantify the loading of therapeutic molecules in various polymeric nanocarriers, including polymer nanoparticles,<sup>[30–35]</sup> amphiphilic copolymer micelles and aggregates,<sup>[36–45]</sup> polyerosomes,<sup>[46–50]</sup> nanogels,<sup>[29,51–54]</sup> polymer brushes,<sup>[55,56]</sup> dendritic core–shell star polymers,<sup>[57]</sup> etc.

### 3.2. Monitoring NCs Formation

FCS can be used not only to characterize preformed NCs, but also to monitor the formation of polymeric nanocarriers such as amphiphilic copolymer micelles or aggregates.<sup>[58–65]</sup> This can be done by testing solutions with increasing concentration of copolymers. To apply FCS at least part of the copolymers needs to be fluorescently labeled. As an example, **Figure 3** shows results obtained by Bonne et al.<sup>[65]</sup> for amphiphilic gradient copolymers P(MOx<sub>40</sub>-g-NOx<sub>6</sub>) that consist of 2-methyl-2-oxazoline (MOx) and 2-nonyl-2-oxazoline (NOx) monomers.

The labeled copolymers' concentration was kept low, at around  $3 \times 10^{-8}$  M. The FCS autocorrelation curves measured at the low overall copolymer concentration could be characterized by a one single diffusing component model (Equation (2),  $m = 1$ ). From the fit the diffusion time the hydrodynamic radius (1.2 nm) of the labeled unimers was obtained. However, above a certain threshold in the overall copolymer concentration an additional ( $m = 2$  in Equation (2)) slower diffusion process appears that originates from large species with a hydrodynamic radius of 4.7 nm, namely, the formed micelles containing both labeled and unlabeled copolymers. From the FCS data one can obtain not only the size of the unimers and the micelles, but also their relative fractions (Figure 3b) and the critical micelle concentration (gray line in Figure 3). This is also a valuable example illustrating the fact that for self-assembled (block) copolymer micelles one should always realize that a certain fraction of non-self-assembled unimeric copolymers are often present.

In a similar way, FCS can be applied to study the formation of other common nanocarriers such as polyplexes or lipoplexes. For example, already in 2001 Rompaey et al.<sup>[66]</sup> used FCS to characterize the complexation between oligonucleotides and cationic polymers. They monitored the formation of polyplexes of rhodamine labeled oligonucleotides and various cationic polymers including

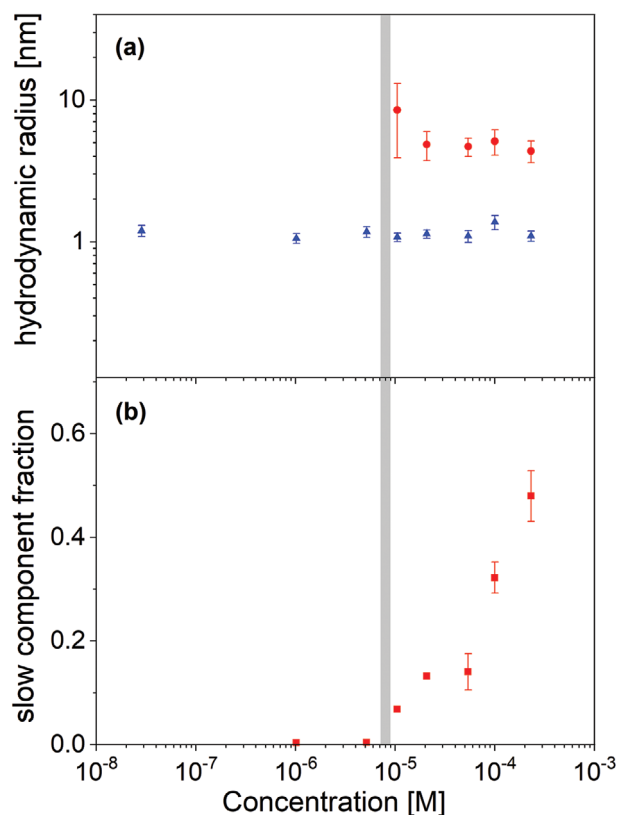


**Figure 3.** Monitoring the micellization of P(MOx40-g-NOx6) gradient copolymers. The studied solutions contained a fraction of fluorescently labeled copolymers with concentration below  $3 \times 10^{-8}$  M. FCS was used to measure the dependence of a) the hydrodynamic radii and b) the relative amplitude of the slow component on the overall copolymer concentration. The gray bar shows the critical micelle concentration (CMC). Adapted with permission.<sup>[65]</sup> Copyright 2007, Wiley-VCH GmbH.

poly(2-dimethylamino)ethyl methacrylate, poly(ethylene glycol)–poly(ethylene imine), and diaminobutane-dendrimer-(NH<sub>2</sub>)<sub>6</sub>4 (DAB64). In the same year, Delie et al.<sup>[30]</sup> used FCS to monitor the formation of another type of NCs, namely, proticles that are agglomerates consisting of oligonucleotides and cationic peptides. By performing experiments on mixtures of rhodamine 6G-labeled 19mer oligonucleotides and protamine (an endogenous, arginine-rich cationic peptide<sup>[67]</sup>) the authors determined the proticles' hydrodynamic diameter and the oligonucleotide:protamine ratio at which all oligonucleotides were complexed. In 2004, Merkle et al.<sup>[68]</sup> applied FCS to study the formation of lipoplexes of a 40 bp oligonucleotide with the cationic lipid, DOTAP. In the last two decades FCS was used extensively to investigate various types of polyplexes<sup>[66,69–79]</sup> and lipoplexes.<sup>[68,80–82]</sup>

### 3.3. Functionalization and Conjugations

The possibility to chemically add and modify single or multiple types of reactive functional groups onto synthetic polymer chain is one of the major advantages to generate functional polymeric nanocarriers compared to other drug delivery systems.

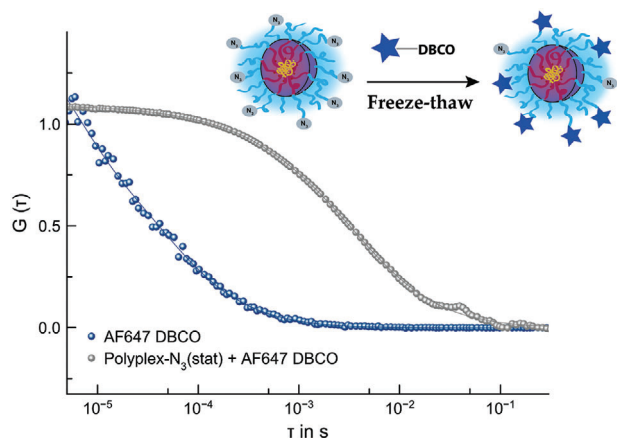


**Figure 4.** Confirming the presence and accessibility of azide-functionalities on the surface of P(Lys)-*b*-P(HPMA)-N<sub>3</sub>(stat) polyplexes by conjugation of AF647-DBCO. Normalized autocorrelation curves measured for freely diffusing AF647 DBCO (blue symbols,  $R_h = 0.75$  nm) and AF647-DBCO conjugated to polyplexes by SPAAC (gray symbols,  $R_h = 52$  nm). Reproduced with permission.<sup>[85]</sup> Copyright 2018, MDPI.

Such groups can be used to conjugate therapeutic molecules, antibodies, fluorescent dyes, etc. or to crosslink the polymers in order to increase NC stability and create stimuli responsive degradation pathways. Due to its sensitivity and selectivity FCS is very well suited to confirm the presence of functional groups on a polymer chain or nanocarrier and to estimate the number of functional groups.<sup>[32,83–86]</sup> Commonly, this is done by monitoring the conjugation of fluorescent molecules bearing an orthogonal reactive group. The conjugation is confirmed in a similar way as the drug loading discussed above—based on the appearance of slowly diffusing species, namely, NCs carrying the conjugated fluorescent molecules. The number of functional groups can be estimated from the number of conjugated fluorescent molecules, which is obtained by dividing the fluorescence brightness of the NCs by that of the fluorescent molecules. For example, Beck et al.<sup>[85]</sup> studied the presence and the accessibility of azide-functionalities on the surface of polyplexes of pDNA and P(Lys)-*b*-P(HPMA)-N<sub>3</sub>(stat) or P(Lys)-*b*-P(HPMA)-N<sub>3</sub>(end) block copolymers. To this end the authors used FCS (**Figure 4**) to confirm the conjugation of a DBCO-containing fluorescent dye (AF 647 DBCO) to the polyplexes by strain-promoted alkyne–azide cycloaddition (SPAAC).

It is important to emphasize that when performing such FCS studies on the interaction between two types of species with significantly different sizes, the small species should be fluorescently labeled. This ensures a significant increase in the size of the fluorescent species upon complexation. On the other hand, if two types of species with similar sizes are studied one can label either of them. This is illustrated in **Figure 5a,b**, which shows respectively the conjugation of a labeled aDEC205 antibody to non-labeled P(Lys)-*b*-P(HPMA)-N<sub>3</sub>(stat) block copolymers and non-labeled aDEC205 antibody to labeled P(Lys)-*b*-P(HPMA)-N<sub>3</sub>(stat) block copolymers.

In many cases, it can be useful to add two or more different types of orthogonal reactive groups onto one NC. The presence and availability of such functional groups on every nanocarrier can be confirmed by monitoring the simultaneous conjugation

of two types of fluorescent molecules bearing the respective orthogonal reactive groups. This can be done by using an extension of the FCS technique, namely, the so-called dual-color fluorescence cross-correlation spectroscopy (dcFCCS).<sup>[87,88]</sup> In a common dcFCCS experiment, the excitation is done by two collinear laser beams with different wavelengths, e.g., “blue” and “red” and the respective fluorescence emissions are detected in two separate channels (**Figure 6a**). This leads to the formation of two overlapping observation volumes (**Figure 6b**).

As “blue” and “red” fluorescence species diffuse through the observation volumes they create fluctuations in the detected fluorescence signals that are monitored and recorded independently (**Figure 6c**). From these intensity fluctuations autocorrelation (AC) and cross-correlation (CC) functions are calculated (**Figure 6d**). If the individual NCs are conjugated with either “blue” or “red” fluorescence molecules only, the respective CC curve will have a low amplitude (**Figure 6d left panel**). By contrast, if all NCs are conjugated with both “red” and “blue” fluorescent molecules the CC curve will have a high amplitude and ideally lie between the two AC curves amplitude (**Figure 6d right panel**).

As an example **Figure 7** shows results of Schäfer et al.<sup>[84]</sup> who synthesized polysarcosine-block-poly(S-alkylsulfonyl)-L-cysteine block copolymers that combine three orthogonal addressable groups: heterotelechelic polypept(o)ides with azide and amine end groups, and a thiolreactive S-alkylsulfonyl cysteine block in the side chain of the polypeptide segment. These block copolymers were used to create multifunctional disulfide core cross-linked nanocarriers with spatially separated functionalities. The authors used the above described dcFCCS approach to confirm the simultaneous attachment of two different dyes on the same nanocarriers (**Figure 7**).

### 3.4. NCs Degradation and Drug Release

FCS can also be applied to study NCs degradation and/or drug release. Here the main advantage of the method is that it can follow these processes in situ without the need for centrifugation or other methods for separation of the (decomposed) NCs and their cargo. As an example, we cite the work of Cabane et al.,<sup>[48]</sup> who studied the UV light induced disintegration of self-assembled poly(methyl caprolactone)-ONB-poly(acrylic acid) (PMCL-ONB-PAA) polymersomes and the simultaneous release of the encapsulated cargo, namely, enhanced green fluorescent protein (eGFP).

**Figure 8** (upper panel) shows typical autocorrelation curves for polymersomes loaded with eGFP measured after increasing amounts of UV irradiation time. The curve measured for the solution of eGFP kept in dark conditions (0 min UV) could be represented by a single component fit (Equation (2),  $m = 1$ ) yielding a value of 230 nm for the hydrodynamic radius of the loaded polymersomes and indicating that there is no freely diffusing, nonencapsulated eGFP. The autocorrelation curves recorded after UV irradiation, have to be fitted by a two component fit (Equation (2),  $m = 2$ ) revealing two populations: free, released GFP and still encapsulated eGFP. From the fits, the fractions of these two populations were estimated. In this way the authors were able to quantitatively follow the NC disintegration and the drug release. **Figure 8** (lower panel) shows the UV irradiation time dependence

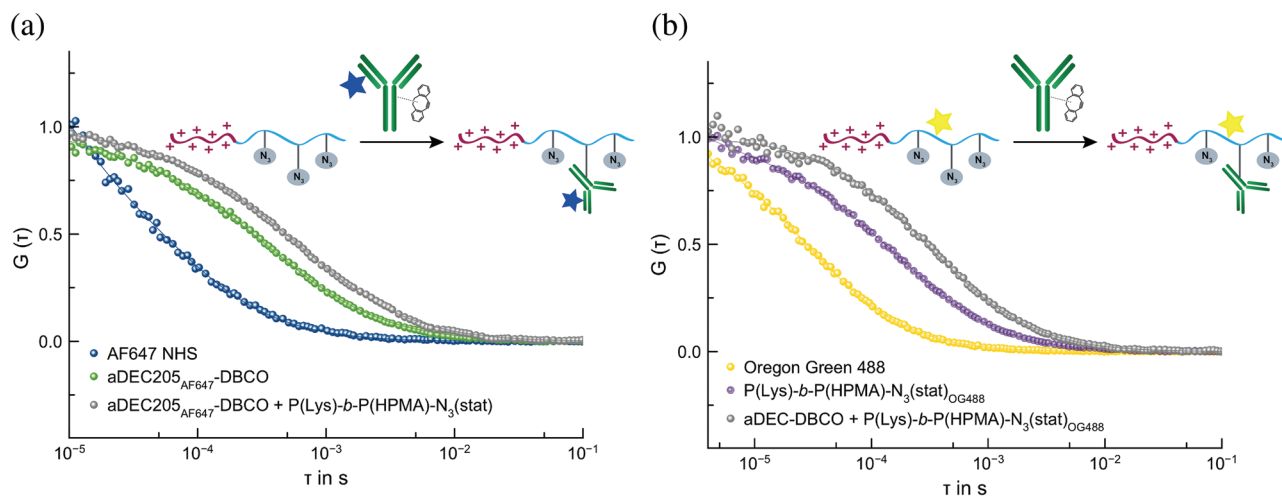


**Figure 5.** Confirming bioconjugations by labeling either the antibody or the copolymer. a) Normalized autocorrelation curves measured for AF647 NHS (blue symbols,  $R_h = 0.76$  nm), aDEC205AF647-DBCO (green symbols,  $R_h = 6.0$  nm) and the conjugate of aDEC205AF647-DBCO and P(Lys)-*b*-P(HPMA)-N<sub>3</sub>(stat) (gray symbols,  $R_h = 10.0$  nm). b) Normalized autocorrelation curves measured for Oregon Green 488 (yellow symbols,  $R_h = 0.58$  nm), P(Lys)-*b*-P(HPMA)-N<sub>3</sub>(stat)<sub>OG488</sub> (purple symbols,  $R_h = 4.3$  nm), and conjugate of aDEC205-DBCO and P(Lys)-*b*-P(HPMA)-N<sub>3</sub>(stat)<sub>OG488</sub> (gray symbols,  $R_h = 10.7$  nm). Reproduced with permission.<sup>[85]</sup> Copyright 2018, MDPI.

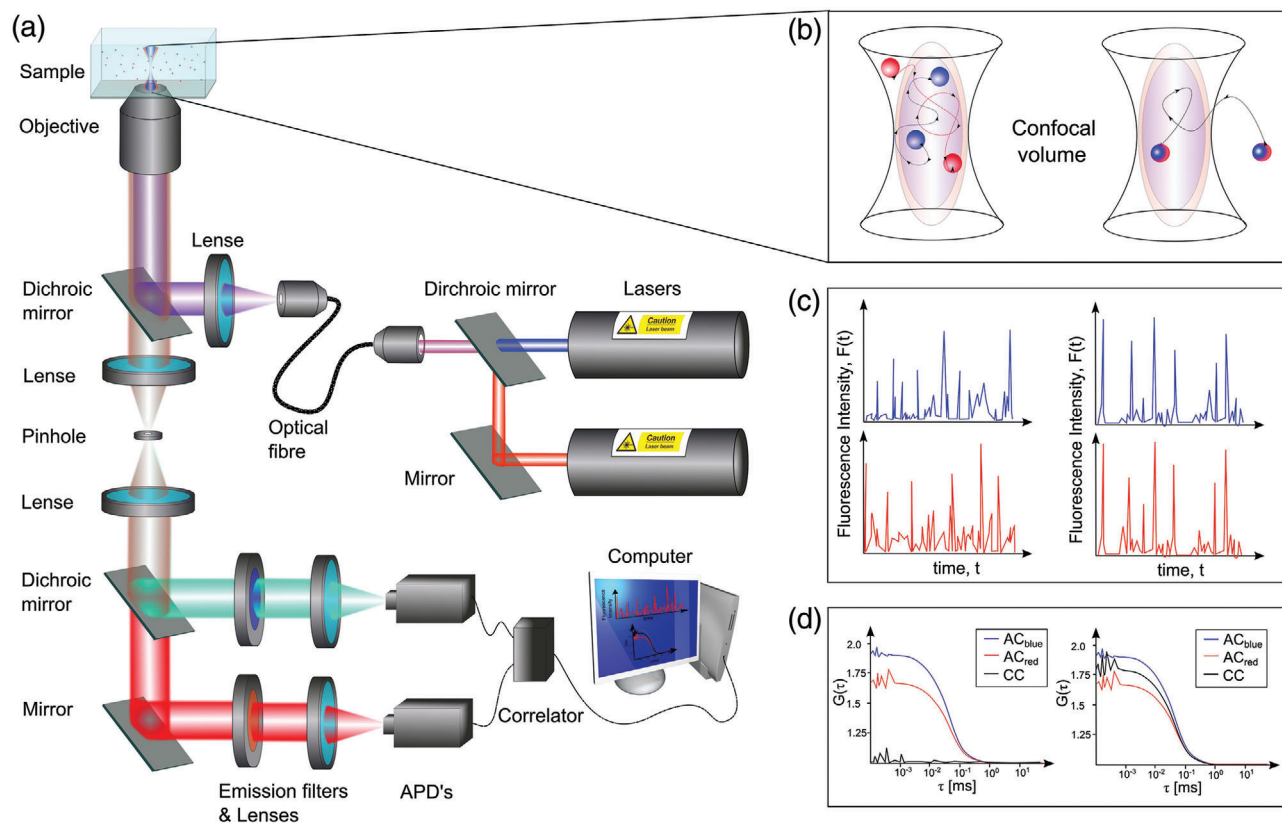


**Figure 6.** a) Schematic representation of a typical dual color FCCS setup. b) Spatially overlapping “blue” and “red” observation volumes are created by the excitation lasers, “blue” and “red” labeled species can diffuse either independently (left) or synchronously (if they associated to each other, right). c) Fluorescence fluctuation and the d) corresponding correlation curves in relation to (b). Reproduced with permission.<sup>[88]</sup> Copyright 2012, American Chemical Society.

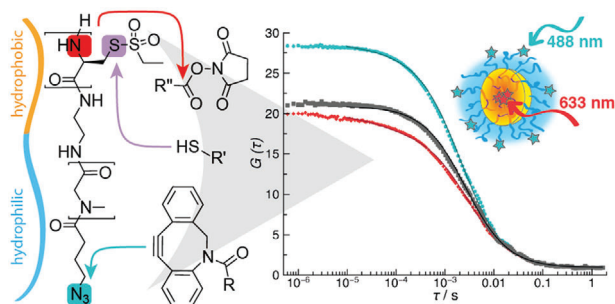


**Figure 7.** Confirming the presence of two types of spatially separated functionalities on a core cross-linked nanocarriers by dual-color fluorescence cross-correlation spectroscopy (dcFCCS). Reproduced with permission.<sup>[84]</sup> Copyright 2012, American Chemical Society.

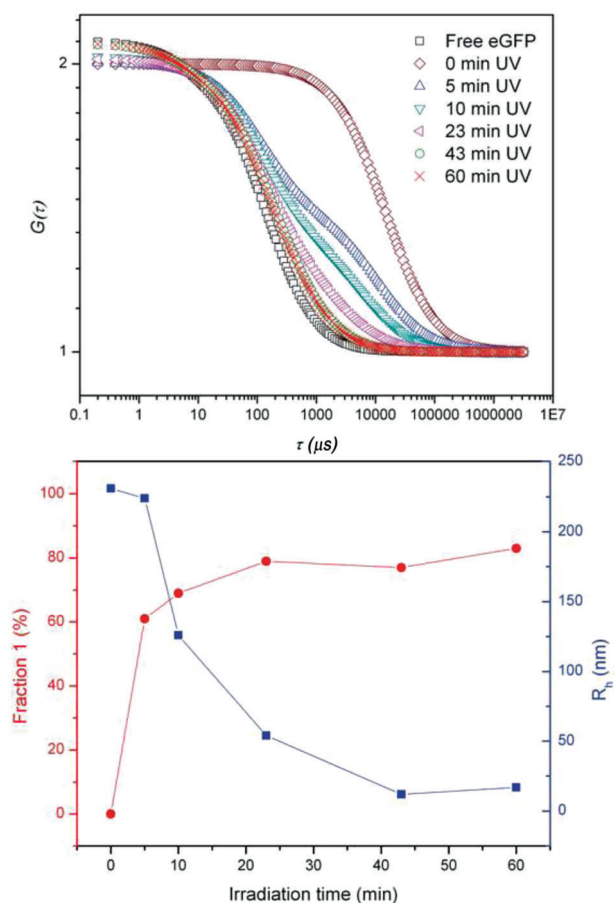


**Figure 8.** Confirming the presence of two types of spatially separated functionalities on a core cross-linked nanoparticles by dual-color fluorescence cross-correlation spectroscopy (dcFCCS). Reproduced with permission.<sup>[48]</sup> Copyright 2011, Royal Society of Chemistry.

on the fraction of released eGFP as well as the hydrodynamic radius of the partially disintegrated supramolecular structures that are still fluorescent due to interactions between eGFP and the PAA chains.

A similar FCS approach was used to study the pH triggered decomposition of hybrid poly(urethane–urea)/silica nanocapsules.<sup>[89]</sup> FCS can also be applied to monitor particle

degradation and cargo release under physiologically relevant triggers during cell uptake. For instance, when mimicking the gradual acidification during endolysosomal particle internalization, an unfolding of ketal-crosslinked squaric ester-derived nanogels could be monitored over time by FCS.<sup>[90]</sup> For siRNA-loaded cationic nanohydrogels, FCS verified the release of the fluorescently labeled cargo upon acidification (for ketal-crosslinked particles) or upon exposure to reductive conditions present in the cytosol (for disulfide-crosslinked particles).<sup>[91,92]</sup>

It should be noted that the fractions of the released cargo and the loaded NCs evaluated from a two-component fit of the experimental autocorrelation curves with Equation (2) (with  $m = 2$ ) should be considered as apparent fractions because they are affected by the fluorescence brightness of the respective components, which is typically significantly higher for the loaded NCs. A detailed discussion on this issue and mathematical approaches needed to obtain the real fractions are discussed by Kristensen et al.<sup>[93]</sup> Furthermore, it should be noted that there are also other approaches to interpret raw FCS data in order to obtain quantitative information on cargo release from nanocarriers. For example, one can avoid autocorrelation analysis altogether and consider only the time dependent intensity fluctuations ( $F(t)$  in Figure 1) measured for solutions containing freely diffusing fluorescent cargo only and solutions in which the cargo is (partially) encapsulated.<sup>[80,81,94]</sup> Alternatively, the standard deviation of  $F(t)$  was also used for the quantitative analysis of dye release from nanocarriers.<sup>[95]</sup>

In another recent study it was suggested<sup>[96]</sup> that the release from liposome-based carriers can be monitored by combining FCS with the use of fluorescein di- $\beta$ -D-galactopyranoside (FDG) and the membrane-impermeable enzyme  $\beta$ -galactosidase ( $\beta$ -Gal). FDG itself is nonfluorescent, and can form fluorescein emitters only in the presence of  $\beta$ -Gal. Thus, as long as FDG is encapsulated in liposomes, no fluorescent signal can be detected. However, if FDG is released, it can be cleaved by  $\beta$ -Gal, and the resulting fluorescence can be characterized, and the levels of release measured with high sensitivity by FCS.<sup>[96]</sup>

## 4. Nanocarriers in Biological Fluids

In order to fulfill their purpose, namely to deliver therapeutic agents to specific tissues and cells, nanocarriers have to be administered such that they come in contact with biological fluids such as saliva, mucus, or blood. The high concentration of cells, numerous proteins, and other components in biological fluids can strongly affect the NCs and cause the formation of a protein corona,<sup>[97,98]</sup> aggregation, decomposition, or premature release of the therapeutic cargo. It is, therefore crucial to study the behavior of the NCs in biological fluids. As discussed below, due to its high sensitivity and fluorescence-based selectivity, the FCS is uniquely suited for such studies.

### 4.1. Protein Corona

Nowadays, it is well established that when a nanoparticle comes into contact with a biological fluid, proteins can adsorb on its surface and form a so-called protein corona.<sup>[98]</sup> However, it should



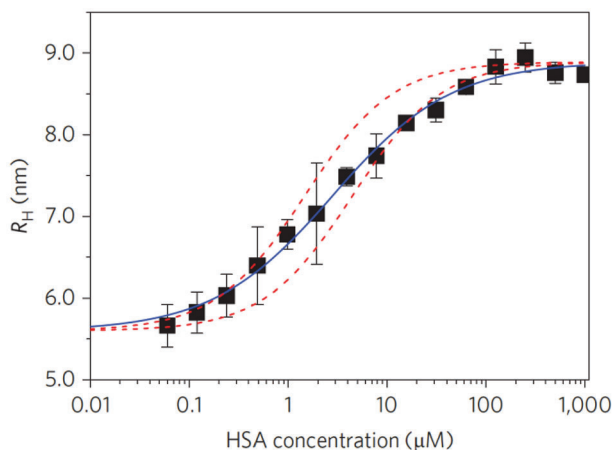


**Figure 9.** FCS studies of the adsorption of HSA on polymer-coated FePt nanoparticles. Dependence of the measured hydrodynamic radii of the particles on the HSA concentration. The experimental data are fitted with either an anti-cooperative binding model (blue solid line) or a Langmuir binding isotherms (red dashed lines) fitted to the first and last 20% of the transition. Reproduced with permission.<sup>[101]</sup> Copyright 2009, Springer Nature.

be, noted that if manufactured properly there are also nanocarriers with neglectable protein corona formation.<sup>[99]</sup> Nevertheless, the formation of a protein corona may be beneficial and can be used to alter the physiological behavior of drug NCs.<sup>[97]</sup> Thus, a variety of experimental methods including FCS have been employed to get insights into the protein corona formation.<sup>[100]</sup> In particular, FCS was applied to investigate protein–nanoparticle interactions under both model (e.g., protein solutions) and physiological (e.g., blood serum) conditions. Here, two main approaches can be considered. If the bare nanoparticles are not significantly larger than the protein corona (about 5–20 nm in diameter), then fluorescent nanoparticles and nonlabeled proteins can be used. One measures an increase in the nanoparticles' hydrodynamic radius upon protein adsorption. As an example, **Figure 9** presents results of the work of Rocker et al.<sup>[101]</sup> who studied the association of human serum albumin (HSA) to polymer-coated, DY-636-labeled FePt nanoparticles. The data show a stepwise increase of the nanoparticle radius of about 3.3 nm, suggesting that HSA molecules form a monolayer around the nanoparticles. In a number of articles from this and other groups,<sup>[101–108]</sup> FCS was used to study the interactions of differently functionalized fluorescently labeled nanoparticles, quantum dots, or gold nanoparticles with nonlabeled proteins. The FCS data allowed an estimation of the equilibrium dissociation constants and yielded information on the orientation of the adsorbed proteins.

While most of these studies were done in solutions of a single type of proteins, recently, Wang et al.<sup>[109]</sup> have extended them also to human blood serum, where the fluorescence-based selectivity of the FCS is especially useful as discussed below.

For nanoparticles that are significantly larger than the plasma proteins, eventual protein adsorption will cause only a minor increase in the measured hydrodynamic radius that can be difficult to detect by FCS. Thus, it is more appropriate to apply FCS using fluorescently labeled proteins.<sup>[110–113]</sup> As FCS monitors only the fluorescent species, the binding of even a single fluorescent

protein to a nonfluorescent nanoparticle will lead to a strong increase in the measured hydrodynamic radius  $R_h$  and can be detected easily. The number of bound proteins can be evaluated by comparing the fluorescence brightness of a nanoparticle–protein complex to that of individual protein molecules. Furthermore, the binding strength can also be estimated by adding competing nonlabeled proteins to the studied solutions.<sup>[110]</sup> On the downside, the need for fluorescent labeling of the proteins hinders the applicability of this type of studies in whole biological fluids. Furthermore, it should be noted that in rare cases labeling can alter the protein properties in a way that may affect their interactions with nanoparticles.<sup>[112]</sup>

#### 4.2. Nanocarrier Stability

The specific properties of the biological fluids may not only lead to formation of protein corona, but they can also affect the stability of the nanocarriers and cause aggregation, decomposition, or premature drug release. FCS experiments have shown that this can happen even in strongly diluted biological fluids. For example, Naito et al.<sup>[114]</sup> studied polyion complexes of anionic siRNA and 3-fluoro-4-carboxyphenylboronic acid modified poly(ethylene glycol)-block-poly(L-lysine) cationic polymers and found that depending on the degree of modification these siRNA nanocarriers can decompose in the presence of 10% fetal bovine serum (FBS). Using FCS the authors were able to accurately measure the diffusion coefficient of the freely diffusing fluorescently labeled siRNA and the loaded NCs in 10% FBS solutions that have essentially the same refractive index and viscosity as pure water.

The situation becomes more complicated when FCS experiments have to be performed in undiluted biological fluids such as blood serum or plasma. In contrast to DLS, FCS is not directly affected by the scattering of large nonfluorescent species that are commonly present in these media. However, FCS results can be affected by the fact that undiluted blood plasma and serum show autofluorescence at some wavelengths and have viscosities and refractive indices higher than those of water. Therefore, in order to obtain reliable quantitative FCS data these factors have to be properly addressed. In particular, one should measure the auto fluorescence intensity under the applied experimental conditions and ensure that it is significantly lower (e.g., ten times) than the average fluorescence intensity in the presence of the studied fluorescent species. The latter can be controlled by tuning the concentration of the studied fluorescent species. In addition, experiments should be performed with a confocal volume positioned as close as possible (e.g., 10–20  $\mu\text{m}$ ) to the cover slide/sample interface to avoid distortions of the FCS observation volume caused by a refractive index mismatch. Finally, when evaluating diffusion coefficients and hydrodynamic radii from the measured diffusion time, one should take into account that the viscosity of blood plasma (serum) is roughly 1.5 times higher than that of water. If these experimental procedures are rigorously applied, FCS can accurately measure even the hydrodynamic radius of individual dye molecules<sup>[56,115]</sup> in undiluted blood plasma. Consequently, the method was applied to study the blood plasma (serum) stability of various nanocarrier

systems including polyplexes,<sup>[79]</sup> branched polymers,<sup>[115–117]</sup> lipid nanoparticles,<sup>[118–120]</sup> nanogels,<sup>[90]</sup> etc.

Alternatively, if no quantitative information on the size of the NCs or released cargo is needed one can evaluate the drug loading stability in undiluted biological fluids<sup>[52,81,94,121]</sup> by considering only the time dependent intensity fluctuations as discussed in Section 3.4. Such approaches are less sensitive on parameters such as refractive index, viscosity, and autofluorescence of the biological fluid.

### 4.3. Nanocarriers Behavior in Whole Blood

In order to reach and accumulate at their intended target sites, systemically administered NCs ideally have to circulate for prolonged periods of time in the blood stream. Therefore, for reliable therapeutic benefits it is of paramount importance that the NCs retain their integrity during circulation. While one can gain some information on the expected fate of the nanocarriers in the blood stream by incubating them externally with, e.g., blood plasma or serum, the best approach will be to characterize the NCs in samples of blood taken from a lab animal or patient at defined time intervals after intravenous administration. However, this is a difficult task, because whole blood is a highly crowded, strongly absorbing and scattering medium. Nevertheless, due to its unique sensitivity and selectivity, the FCS technique is capable of tracking the fate of nanocarriers under the challenging conditions in the blood stream and can be applied for such studies using several approaches of increasing complexities.

For example, Watanabe et al.<sup>[122]</sup> studied the blood stream stability of so-called unit polyion complexes (uPIC). These are dynamic ion-pairs of single siRNA molecules with Y-shaped block cationomers of precisely regulated chain lengths where the number of positive charges perfectly matches with the negative charges of each oligonucleotide strand. uPICs containing Alexa 647 labeled siRNA were injected in mice and 500  $\mu\text{L}$  of blood was harvested 60 min later. The blood sample was then centrifuged to obtain blood plasma that was diluted ten times with PBS in order to adjust the fluorescence intensity to the detection range appropriate for the FCS analysis. Using this approach, the authors were able not only to confirm that the uPICs retain their size of about 18 nm after 60 min circulation in the blood stream, but also to show that stable uPICs can be formed directly in blood if the two components are injected separately.<sup>[122]</sup>

In another example, Tiiman et al.<sup>[123]</sup> applied FCS to identify the presence of structured amyloidogenic oligomeric aggregates in blood serum of patients with Alzheimer's disease and found that both the size and the concentration of the nanoplaques are higher than in control individuals. To enable fluorescence detection of the aggregates, the authors added the benzothiazole salt Thioflavin T (ThT) to the studied blood serum samples and used the fact that ThT binds to the aggregates and as a result significantly changes its spectral properties for selective fluorescent detection.

The two studies discussed above share the need of centrifugation in order to remove the blood cells and obtain plasma and serum that can afterward be studied by FCS. However, it should be realized that the centrifugation creates strong shear forces that can potentially cause aggregation, decomposition, or loss

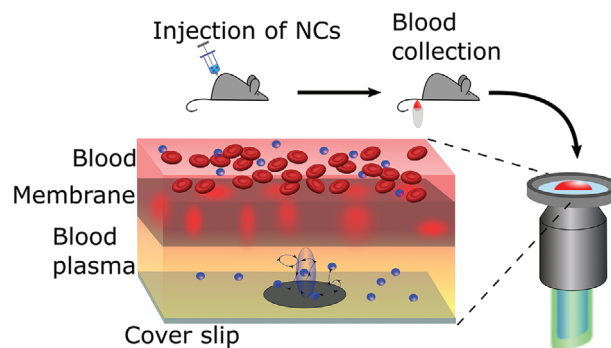


**Figure 10.** Schematic representation of the FCS experiments with droplets of blood. Reproduced with permission.<sup>[124]</sup> Copyright 2022, American Chemical Society.

of drug cargo, particularly in soft nanocarriers such as micelles, nanogels, lipoplexes or polyplexes. Furthermore, centrifugation requires relatively large amounts of blood ( $\approx\text{mL}$  quantities) that cannot be obtained multiple times from a single mouse and it can be invasive for patients. To avoid these problems, we recently suggested<sup>[124]</sup> an alternative FCS approach that allows characterization of NCs using blood samples of less than 50  $\mu\text{L}$ . Instead of applying centrifugation, the blood plasma can be obtained in situ by placing a small piece of plasma separation membrane (supported by a spacer) directly above the microscope coverslip of the FCS sample chamber (**Figure 10**). The confocal detection volume is positioned in the space between the microscope coverslip and the membrane. A blood droplet of about 30  $\mu\text{L}$  is placed on the membrane. The large blood cells are retained by the membrane, but the liquid part of the blood and the NCs can pass through and reaches the detection volume (**Figure 10**), thus enabling standard FCS characterization. We applied this method to follow the size, concentration, and loading efficiency of pH-degradable fluorescent cargo-loaded nanogels in the blood of live mice for periods of up to 72 h.

More complex approaches allow monitoring of drug nanocarriers and their cargo in whole blood samples without removing the blood cells. Recently, we<sup>[56]</sup> studied drug NCs' size, stability, premature drug release, and interaction with proteins directly in samples of whole blood. The NCs and/or their cargo were labeled with dye molecules that have absorption and emission wavelengths in the near-infrared (NIR) range from 700 to 1000 nm, which is associated with the so-called biological window. This allowed to decrease the absorption of both excitation and emission light from the blood. Furthermore, the FCS experiments were performed during a very slow continuous flow of the studied blood sample through a microchannel, in order to ensure time intervals in which the FCS detection volume will be free of blood cells (**Figure 11**, left panel).

The measured autocorrelation curves were fitted by a complex model that includes diffusion and flow terms and combines normal and inverted FCS<sup>[125]</sup> in order to account for the effect of the blood cells crossing the FCS observation volume.<sup>[56]</sup> Using this approach we were able to detect even individual NIR dye molecules in whole blood samples. Furthermore, we studied the blood stability of polypept(o)ides-based core-crosslinked micelles loaded with an NIR dye (IRDye800CW) as a model for

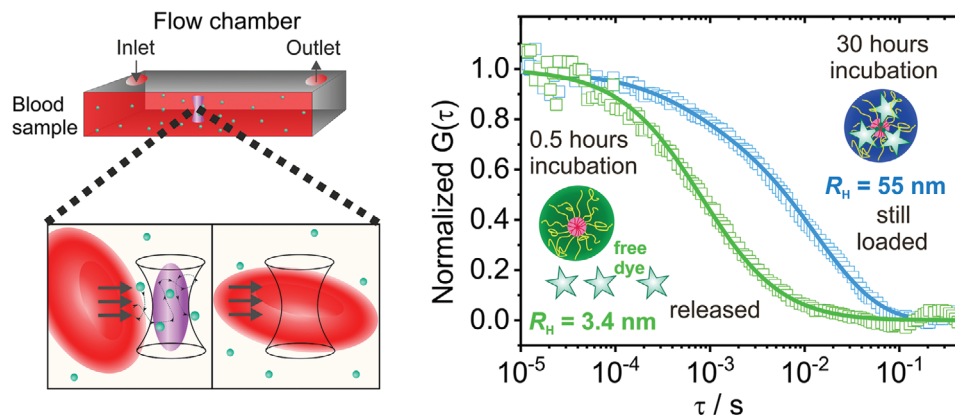


**Figure 11.** (Left panel) Schematic representation of the NIR-FCS experiments in flowing blood. The FCS observation volume is consequently either free (left) or occupied (right) by a blood cell. (Right panel) Normalized autocorrelation curves measured in human blood for core-crosslinked micelles that were either covalently (blue color) or noncovalently (green color) loaded with IRDye800CW. The dye incubation in blood was done at 4 °C. Adapted with permission.<sup>[56]</sup> Copyright 2018, Springer Nature.

small molecular weight drug. While covalently loaded dyes were still attached to the NCS even after 30 h incubation in blood, hydrophobically loaded dyes were fully released after only 30 min (Figure 11, right panel).

In another interesting recent development, Fu et al.<sup>[126]</sup> applied multiphoton FCS in vivo to quantify cerebral blood flow in thinned-skulled live mice using fluorescently labeled polymer nanoparticles as tracers. In addition to the flow profiling, the authors were able to obtain some qualitative information on changes in the nanoparticle concentration and on the dissociation of fluorophores from the nanoparticles. Due to the limitations of the applied simplified FCS data processing method imposed by the high flow rates in the blood vessels, the obtained results still lack the quantitative accuracy needed for precise characterization of drug NCs and their cargo. Nevertheless, the reported FCS experiment bears promises for further developments toward accurate in vivo characterization of NCs in the blood stream of rodents and other animals.

## 5. Nanocarriers in Living Cells

As a final step in NC drug delivery, NCs need to release their drug cargo, for instance into the cytoplasm of target cells. However, monitoring this process is a difficult task due to the very small sizes of the NCs and the drug molecules on the one hand and the larger, but still small and complex live cells on the other hand. These challenges can still be addressed by using FCS. One of the most prominent and unique characteristics of the FCS is its very small observation volume ( $\approx 0.2 \mu\text{m}^3$ ). This volume can be positioned anywhere within a cell with a spatial precision of 0.5  $\mu\text{m}$ , thus making the FCS a perfect tool to study dynamic processes in living cells.<sup>[20,127–143]</sup> In one of the first studies in 1995, Berland et al.<sup>[144]</sup> used two photon FCS to measure the diffusion coefficients of small latex beads (7 and 15 nm radius) in the cytoplasm of mouse fibroblast cells. They found that the beads diffuse two to five times slower in cytoplasm than in water due to the higher viscosity and eventual binding of the beads to cellular components. In 1998, Politz et al.<sup>[145]</sup> applied FCS to study the intracellular diffusion of oligonucleotides and even observed their hybridization

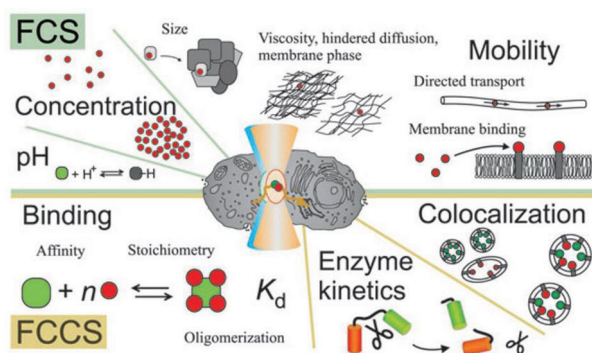


**Figure 12.** Overview of relevant intracellular applications of fluorescence autocorrelation (top) and cross-correlation (bottom) spectroscopy. Particle concentration and mobility can be determined by FCS (top), but especially for particle mobility one should take into account its size, the viscosity of the surrounding phase, and further obstacles therein. Beyond free Brownian diffusion a directed transport can be identified by analysis of the shape of the autocorrelation curve. Moreover, by analysis of its “blinking”—a result of reversible protonation occurring in the chromophore—the eGFP protein can be used as a pH indicator. For FCCS (bottom), the resulting cross-correlation amplitudes in conjunction with the autocorrelation amplitudes can reveal information on respective binding partners, enzyme kinetics or dynamic colocalization. Reproduced with permission.<sup>[147]</sup> Copyright 2006, Springer Nature.

with polyadenylated RNA in the nuclei of rat myoblasts. Already in these early studies, it becomes clear that there are significant variations in the measured diffusion rates depending on characteristics of individual cells and cell (nuclei) regions. This factor, together with the possible binding to unknown cell components and the presence of autofluorescence,<sup>[146]</sup> makes the quantitative evaluation of FCS data measured in living cells more challenging than in aqueous solution or in blood (plasma). As discussed by Bacia et al.,<sup>[147]</sup> the use of the dual colored version of FCS, the FCCS may help significantly to get more precise information in particular when studying binding, enzyme kinetics or colocalization (Figure 12).

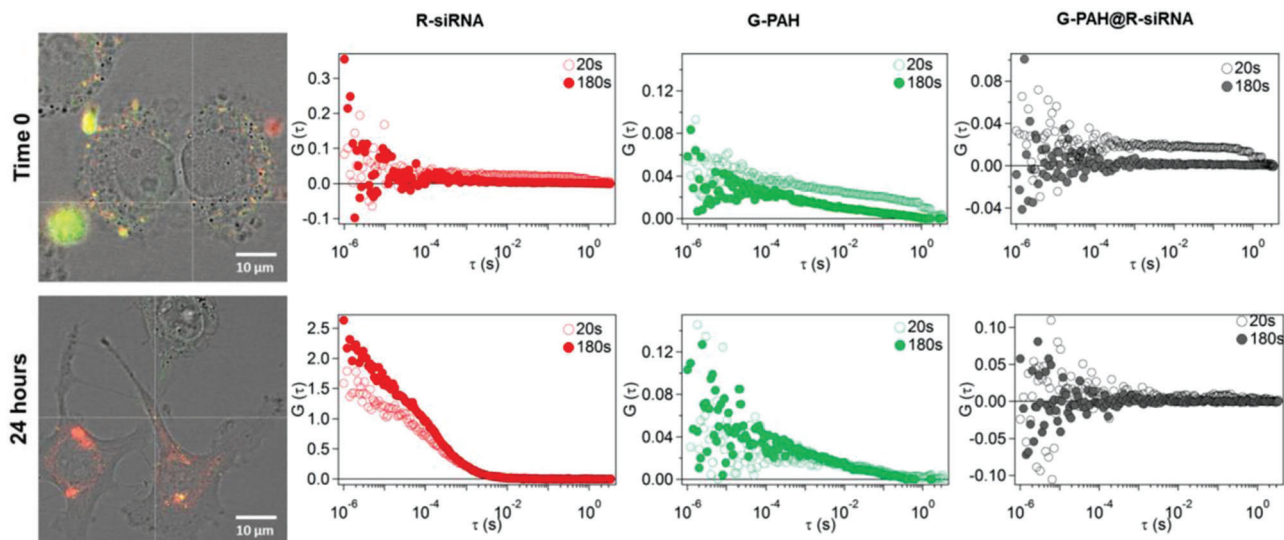


**Figure 13.** FCS experiments in live A549 cells incubated with PAH–siRNA polyplexes. Images and FCS data were acquired immediately (Time 0), and after 24 h incubation at 37 °C and 5% CO<sub>2</sub>. The autocorrelation functions in the red and the green channels are associated with siRNA and PAH, respectively. The cross-correlation function (black symbols) is associated with PAH/siRNA polyplexes. Each location was measured in 20 runs of 10 s each. Average curves are reported after 20s and 180s to elucidate bleaching effects. Reproduced with permission.<sup>[148]</sup> Copyright 2019, Elsevier.

All these considerations are certainly valid for FCS studies analyzing an intracellular cargo release from NCs. In general, if the cargo molecules are fluorescently labeled, one can monitor their release by the appearance of a subfraction of faster diffusing species in the confocal volume, namely, the released cargo molecules. However, shortly after release these molecules may interact with cell components and desired binding partners and thereby, significantly change their diffusion coefficient. Therefore, in order to get more accurate information on the release it is helpful to fluorescently label (with different dyes) both the cargo molecules and the NCs and monitor their colocalization with FCCS. For example, Di Silvio et al.<sup>[148]</sup> used this approach to study the fate of poly(allylamine hydrochloride) (PAH)–siRNA polyplexes after uptake in A549 cells. The PAH molecules were labeled with rhodamine and the siRNA with Cy5. It was observed that 24 h after uptake both the cross-correlation between PAH and siRNA channels and the diffusion times measured in the siRNA channel decreased substantially indicating disassembly of the polyplexes and release of the siRNA (**Figure 13**).

More details on the FCS specifics, advantages and shortcomings can be found in a comprehensive report<sup>[149]</sup> by De Smedt and co-workers, who have extensively applied FCS<sup>[150,151]</sup> to study the intracellular behavior of DNA nanoparticles, in particular with respect to protection of the nucleic acids against enzymatic degradation and their release from the nanocarriers.

## 6. Conclusions

During the last two decades fluorescence correlation spectroscopy has become an extremely useful tool, helping scientists to follow the fate of polymeric drug nanocarriers at all stages of the drug delivery process. Due to its noninvasive nature, single molecule sensitivity, selectivity, and small probing volume, the method can monitor NCs formation, degradation, drug loading

and release—even in complex biological environments in vitro and in vivo.

Such studies are not limited to polymeric NCs, but can also be applied to other nanocarrier system. In particular, nanocarriers based on lipids<sup>[40,68,81,95,96,152–156]</sup> and proteins<sup>[157–160]</sup> as well as on metal–organic framework,<sup>[86,161,162]</sup> calcium phosphate,<sup>[163,164]</sup> silica<sup>[165–167]</sup> or gold<sup>[168,169]</sup> nanoparticles, were often characterized with FCS. Furthermore, inherently fluorescent nanoparticles such as quantum dots,<sup>[101,104,109,170–172]</sup> carbon dots<sup>[173–175]</sup> or nanodiamonds<sup>[176–179]</sup> have been extensively studied with respect to their interactions with plasma proteins and use for transfection or bioimaging.

Despite its numerous advantages, FCS has also limitations, most importantly the need for fluorescent labeling. This however, is partially compensated by the availability of well-established labeling protocols. Furthermore, it is clear that no experimental method can provide a comprehensive picture of the fate of the NCs during the entire delivery processes. Thus, in this endeavor FCS studies strongly benefit from a combination with complementary methods such as dynamic light scattering, size exclusion chromatography, transmission electron microscopy, Rahman microscopy, confocal laser scanning microscopy, flow cytometry, fluorescence recovery after photobleaching, fluorescence imaging, magnetic resonance imaging, positron emission tomography, etc.

In perspective, we believe that the use of FCS in the drug NCs development will grow further, promoted not only by the unique characteristics of the method, but also by the increasing availability of the FCS equipment, which nowadays is an almost standard part of any commercial confocal microscope. In combination with other methods, FCS will be providing a detailed molecular characterization that can reveal in depth information on the behavior of the NCs and their cargo, that is especially relevant for mechanistic studies and for translational purposes. Furthermore, based on the developments in intravital microscopy of

animal models we expect that FCS may become a significant tool for translational in vivo monitoring of drug NCs toward a comprehensive understanding of their therapeutic performance.

## Acknowledgements

The financial support of the DFG through the SFB 1066 projects Q02, B03 and B04 as well as the Emmy Noether program to L.N. is gratefully acknowledged.

Open access funding enabled and organized by Projekt DEAL.

## Conflict of Interest

The authors declare no conflict of interest.

## Keywords

drug delivery, fluorescence correlation spectroscopy, polymeric nanocarriers

Received: December 16, 2021

Revised: February 4, 2022

Published online: March 7, 2022

- [1] H. Ringsdorf, *J. Polym. Sci., Part C: Polym. Symp.* **1975**, 51, 135.
- [2] R. Duncan, R. Gaspar, *Mol. Pharm.* **2011**, 8, 2101.
- [3] R. A. Petros, J. M. DeSimone, *Nat. Rev. Drug Discovery* **2010**, 9, 615.
- [4] S. Grabbe, H. Haas, M. Diken, L. M. Kranz, P. Langguth, U. Sahin, *Nanomedicine* **2016**, 11, 2723.
- [5] A. L. P. Silvestre, J. A. Oshiro, C. Garcia, B. O. Turco, J. M. D. Leite, B. Damasceno, J. C. M. Soares, M. Chorilli, *Curr. Med. Chem.* **2021**, 28, 401.
- [6] U. Sahin, P. Oehm, E. Derhovanessian, R. A. Jabulowsky, M. Vormehr, M. Gold, D. Maurus, D. Schwarck-Kokarakis, A. N. Kuhn, T. Omokoko, L. M. Kranz, M. Diken, S. Kreiter, H. Haas, S. Attig, R. Rae, K. Cuk, A. Kemmer-Bruck, A. Breitkreuz, C. Tolliver, J. Caspar, J. Quinkhardt, L. Hebich, M. Stein, A. Hohberger, I. Vogler, I. Liebig, S. Renken, J. Sikorski, M. Leierer, et al., *Nature* **2020**, 585, 107.
- [7] A. B. Vogel, I. Kanevsky, Y. Che, K. A. Swanson, A. Muik, M. Vormehr, L. M. Kranz, K. C. Walzer, S. Hein, A. Guler, J. Loschko, M. S. Maddur, A. Ota-Setlik, K. Tompkins, J. Cole, B. G. Lui, T. Ziegenhals, A. Plaschke, D. Eisel, S. C. Dany, S. Fesser, S. Erbar, F. Bates, D. Schneider, B. Jesionek, B. Sanger, A. K. Wallisch, Y. Feuchter, H. Junginger, S. A. Krumm, et al., *Nature* **2021**, 592, 283.
- [8] M. J. Mitchell, M. M. Billingsley, R. M. Haley, M. E. Wechsler, N. A. Peppas, R. Langer, *Nat. Rev. Drug Discovery* **2021**, 20, 101.
- [9] E. B. Manaia, M. P. Abucafy, B. G. Chiari-Andreo, B. L. Silva, J. A. Oshiro, L. A. Chiavacci, *Int. J. Nanomed.* **2017**, 12, 4991.
- [10] P. M. Perrigue, R. A. Murray, A. Mielcarek, A. Henschke, S. E. Moya, *Pharmaceutics* **2021**, 13.
- [11] D. Magde, W. W. Webb, E. Elson, *Phys. Rev. Lett.* **1972**, 29, 705.
- [12] E. L. Elson, D. Magde, *Biopolymers* **1974**, 13, 1.
- [13] D. Magde, E. L. Elson, W. W. Webb, *Biopolymers* **1974**, 13, 29.
- [14] H. Qian, E. L. Elson, *Appl. Opt.* **1991**, 30, 1185.
- [15] R. Rigler, U. Mets, J. Widengren, P. Kask, *Eur. Biophys. J.* **1993**, 22, 169.
- [16] M. Eigen, R. Rigler, *Proc. Natl. Acad. Sci. USA* **1994**, 91, 5740.
- [17] R. Rigler, E. Elson, *Fluorescence Correlation Spectroscopy: Theory and Applications*, Springer, Berlin **2001**.
- [18] S. T. Hess, S. H. Huang, A. A. Heikal, W. W. Webb, *Biochemistry* **2002**, 41, 697.
- [19] M. A. Medina, P. Schwille, *BioEssays* **2002**, 24, 758.
- [20] S. A. Kim, P. Schwille, *Curr. Opin. Neurobiol.* **2003**, 13, 583.
- [21] S. A. Kim, K. G. Heinze, P. Schwille, *Nat. Methods* **2007**, 4, 963.
- [22] T. A. Yu, M. M. Martinez, D. Pappas, *Appl. Spectrosc.* **2011**, 65, 115A.
- [23] K. Koynov, H. J. Butt, *Curr. Opin. Colloid Interface Sci.* **2012**, 17, 377.
- [24] D. Woll, *RSC Adv.* **2014**, 4, 2447.
- [25] C. M. Papadakis, P. Kosovan, W. Richtering, D. Woll, *Colloid Polym. Sci.* **2014**, 292, 2399.
- [26] A. Gupta, J. Sankaran, T. Wohland, *Phys. Sci. Rev.* **2019**, 4, 20170104.
- [27] X. Z. Zhang, A. Poniewierski, K. Sozanski, Y. Zhou, A. Brzozowska-Elliott, R. Holyst, *Phys. Chem. Chem. Phys.* **2019**, 21, 1572.
- [28] I. De Santo, L. Sanguigno, F. Causa, T. Monetta, P. A. Netti, *Analyst* **2012**, 137, 5076.
- [29] L. Nuhn, M. Hirsch, B. Krieg, K. Koynov, K. Fischer, M. Schmidt, M. Helm, R. Zentel, *ACS Nano* **2012**, 6, 2198.
- [30] F. Delie, R. Gurny, A. Zimmer, *Biol. Chem.* **2001**, 382, 487.
- [31] J. Weyermann, D. Lochmann, C. Georgens, I. Rais, J. Kreuter, M. Karas, M. Wolkenhauer, A. Zimmer, *Eur. J. Pharm. Biopharm.* **2004**, 58, 25.
- [32] P. Rigler, W. Meier, *J. Am. Chem. Soc.* **2006**, 128, 367.
- [33] L. Florez, C. Herrmann, J. M. Cramer, C. P. Hauser, K. Koynov, K. Landfester, D. Crespy, V. Mailander, *Small* **2012**, 8, 2222.
- [34] E. Aschenbrenner, K. Bley, K. Koynov, M. Makowski, M. Kappl, K. Landfester, C. K. Weiss, *Langmuir* **2013**, 29, 8845.
- [35] V. Beer, K. Koynov, W. Steffen, K. Landfester, A. Musyanovych, *Macromol. Chem. Phys.* **2015**, 216, 1774.
- [36] M. Barz, F. K. Wolf, F. Canal, K. Koynov, M. J. Vicent, H. Frey, R. Zentel, *Macromol. Rapid Commun.* **2010**, 31, 1492.
- [37] M. Hemmelmann, C. Knoth, U. Schmitt, M. Allmeroth, D. Moderegger, M. Barz, K. Koynov, C. Hiemke, F. Rosch, R. Zentel, *Macromol. Rapid Commun.* **2011**, 32, 712.
- [38] M. Barz, A. Arminan, F. Canal, F. Wolf, K. Koynov, H. Frey, R. Zentel, M. J. Vicent, *J. Controlled Release* **2012**, 163, 63.
- [39] M. Allmeroth, D. Moderegger, D. Gundel, H. G. Buchholz, N. Mohr, K. Koynov, F. Rosch, O. Thews, R. Zentel, *J. Controlled Release* **2013**, 172, 77.
- [40] S. Draffehn, J. Eichhorst, B. Wiesner, M. U. Kunkel, *Langmuir* **2016**, 32, 6928.
- [41] S. Florinas, M. Liu, R. Fleming, L. Van Vlerken-Ysla, J. Ayriss, R. Gilbreth, N. Dimasi, C. Gao, H. Wu, Z. Q. Xu, S. Chen, A. Dirisala, K. Kataoka, H. Cabral, R. J. Christie, *Biomacromolecules* **2016**, 17, 1818.
- [42] A. Tao, G. L. Huang, K. Igarashi, T. Hong, S. Liao, F. Stellacci, Y. Matsumoto, T. Yamasoba, K. Kataoka, H. Cabral, *Macromol. Biosci.* **2020**, 20, 1900161.
- [43] H. S. Min, H. J. Kim, M. Naito, S. Ogura, K. Toh, K. Hayashi, B. S. Kim, S. Fukushima, Y. Anraku, K. Miyata, K. Kataoka, *Angew. Chem., Int. Ed. Engl.* **2020**, 59, 8173.
- [44] D. Gonzalez-Carter, X. Liu, T. A. Tockary, A. Dirisala, K. Toh, Y. Anraku, K. Kataoka, *Proc. Natl. Acad. Sci. USA* **2020**, 117, 19141.
- [45] R. Kembaren, R. Fokkink, A. H. Westphal, M. Kamperman, J. M. Kleijn, J. W. Borst, *Langmuir* **2020**, 36, 8494.
- [46] W. Mueller, K. Koynov, S. Pierrat, R. Thiermann, K. Fischer, M. Maskos, *Polymer* **2011**, 52, 1263.
- [47] W. Mueller, K. Koynov, K. Fischer, S. Hartmann, S. Pierrat, T. Basche, M. Maskos, *Macromolecules* **2009**, 42, 357.
- [48] E. Cabane, V. Malinova, S. Menon, C. G. Palivan, W. Meier, *Soft Matter* **2011**, 7, 9167.
- [49] Y. Anraku, A. Kishimura, M. Kamiya, S. Tanaka, T. Nomoto, K. Toh, Y. Matsumoto, S. Fukushima, D. Sueyoshi, M. R. Kano, Y. Urano, N. Nishiyama, K. Kataoka, *Angew. Chem., Int. Ed. Engl.* **2016**, 55, 560.
- [50] D. Sueyoshi, Y. Anraku, T. Komatsu, Y. Urano, K. Kataoka, *Biomacromolecules* **2017**, 18, 1189.

- [51] K. Raemdonck, B. Naeye, K. Buyens, R. E. Vandenbroucke, A. Hogset, J. Demeester, S. C. De Smedt, *Adv. Funct. Mater.* **2009**, *19*, 1406.
- [52] B. Naeye, H. Deschout, M. Roding, M. Rudemo, J. Delanghe, K. Devreese, J. Demeester, K. Braeckmans, S. C. De Smedt, K. Raemdonck, *Biomaterials* **2011**, *32*, 9120.
- [53] L. De Backer, K. Braeckmans, M. C. Stuart, J. Demeester, S. C. De Smedt, K. Raemdonck, *J. Controlled Release* **2015**, *206*, 177.
- [54] Y. Sasaki, D. Iida, H. Takahashi, S.-I. Sawada, K. Akiyoshi, *Curr. Drug Discovery Technol.* **2011**, *8*, 308.
- [55] J. Buhler, S. Gietzen, A. Reuter, C. Kappel, K. Fischer, S. Decker, D. Schafel, K. Koynov, M. Bros, I. Tubbe, S. Grabbe, M. Schmidt, *Chem. - Eur. J.* **2014**, *20*, 12405.
- [56] I. Negwer, A. Best, M. Schinnerer, O. Schafer, L. Capeloa, M. Wagner, M. Schmidt, V. Mailander, M. Helm, M. Barz, H. J. Butt, K. Koynov, *Nat. Commun.* **2018**, *9*, 5306.
- [57] M. Yin, C. R. W. Kuhlmann, K. Sorokina, C. Li, G. Mihov, E. Pietrowski, K. Koynov, M. Klapper, H. J. Luhmann, K. Müllen, T. Weil, *Biomacromolecules* **2009**, *9*, 1381.
- [58] M. Barz, F. Canal, K. Koynov, R. Zentel, M. a. J. Vicent, *Biomacromolecules* **2010**, *11*, 2274.
- [59] M. Allmeroth, D. Moderegger, B. Biesalski, K. Koynov, F. Rosch, O. Thews, R. Zentel, *Biomacromolecules* **2011**, *12*, 2841.
- [60] M. Hemmelmann, D. Kurzbach, K. Koynov, D. Hinderberger, R. Zentel, *Biomacromolecules* **2012**, *13*, 4065.
- [61] M. Hemmelmann, V. V. Metz, K. Koynov, K. Blank, R. Postina, R. Zentel, *J. Controlled Release* **2012**, *163*, 170.
- [62] S. K. Filippov, P. Chytil, P. V. Konarev, M. Dyakonova, C. Papadakis, A. Zhigunov, J. Plestil, P. Stepanek, T. Etrych, K. Ulbrich, D. I. Svergun, *Biomacromolecules* **2012**, *13*, 2594.
- [63] M. Allmeroth, D. Moderegger, D. Gundel, K. Koynov, H. G. Buchholz, K. Mohr, F. Rosch, R. Zentel, O. Thews, *Biomacromolecules* **2013**, *14*, 3091.
- [64] T. B. Bonne, K. Ludtke, R. Jordan, P. Stepanek, C. M. Papadakis, *Colloid Polym. Sci.* **2004**, *282*, 833.
- [65] T. B. Bonne, K. Ludtke, R. Jordan, C. M. Papadakis, *Macromol. Chem. Phys.* **2007**, *208*, 1402.
- [66] E. V. Rompaey, Y. Engelborghs, N. Sanders, S. C. D. Smedt, J. Demeester, *Pharm. Res.* **2001**, *18*, 928.
- [67] I. Ruseska, K. Fresacher, C. Petschacher, A. Zimmer, *Nanomaterials* **2021**, *11*, 1508.
- [68] D. Merkle, S. P. Lees-Miller, D. T. Cramb, *Biochemistry* **2004**, *43*, 7263.
- [69] T. Miyazaki, S. Uchida, S. Nagatoishi, K. Koji, T. Hong, S. Fukushima, K. Tsumoto, K. Ishihara, K. Kataoka, H. Cabral, *Adv. Healthcare Mater.* **2020**, *9*, 2000538.
- [70] W. Yang, T. Miyazaki, P. Chen, T. Hong, M. Naito, Y. Miyahara, A. Matsumoto, K. Kataoka, K. Miyata, H. Cabral, *Sci. Technol. Adv. Mater.* **2021**, *22*, 850.
- [71] B. Krieg, M. Hirsch, E. Scholz, L. Nuhn, I. Tabujew, H. Bauer, S. Decker, A. Khobta, M. Schmidt, W. Tremel, R. Zentel, K. Peneva, K. Koynov, A. J. Mason, M. Helm, *Pharm. Res.* **2015**, *32*, 1957.
- [72] I. Tabujew, C. Freidel, B. Krieg, M. Helm, K. Koynov, K. Mullen, K. Peneva, *Macromol. Rapid Commun.* **2014**, *35*, 1191.
- [73] I. Tabujew, M. Heidari, C. Freidel, M. Helm, L. Tebbe, U. Wolfrum, K. Nagel-Wolfrum, K. Koynov, P. Biehl, F. H. Schacher, R. Potestio, K. Peneva, *Biomacromolecules* **2019**, *20*, 4389.
- [74] I. Tabujew, M. Willig, N. Leber, C. Freidel, I. Negwer, K. Koynov, M. Helm, K. Landfester, R. Zentel, K. Peneva, V. Mailander, *Acta Biomater.* **2019**, *100*, 338.
- [75] K. Tappertzhofen, S. Beck, E. Montermann, D. Huesmann, M. Barz, K. Koynov, M. Bros, R. Zentel, *Macromol. Biosci.* **2016**, *16*, 106.
- [76] J. DeRouchey, C. Schmidt, G. F. Walker, C. Koch, C. Plank, E. Wagner, J. O. Radler, *Biomacromolecules* **2008**, *9*, 724.
- [77] J. DeRouchey, G. F. Walker, E. Wagner, J. O. Radler, *J. Phys. Chem. B* **2006**, *110*, 4548.
- [78] C. Troiber, D. Edinger, P. Kos, L. Schreiner, R. Klager, A. Herrmann, E. Wagner, *Biomaterials* **2013**, *34*, 1624.
- [79] C. Troiber, J. C. Kasper, S. Milani, M. Scheible, I. Martin, F. Schaubhut, S. Kuchler, J. Radler, F. C. Simmel, W. Friess, E. Wagner, *Eur. J. Pharm. Biopharm.* **2013**, *84*, 255.
- [80] T. Furst, G. R. Dakwar, E. Zagato, A. Lechanteur, K. Remaut, B. Evrard, K. Braeckmans, G. Piel, *J. Controlled Release* **2016**, *236*, 68.
- [81] K. Buyens, B. Lucas, K. Raemdonck, K. Braeckmans, J. Vercommen, J. Hendrix, Y. Engelborghs, S. C. De Smedt, N. N. Sanders, *J. Controlled Release* **2008**, *126*, 67.
- [82] G. R. Dakwar, K. Braeckmans, W. Ceelen, S. C. De Smedt, K. Remaut, *Drug Delivery Transl. Res.* **2017**, *7*, 241.
- [83] K. Qi, Q. Ma, E. E. Remsen, Christopher, G. J. Clark, K. L. Wooley, *J. Am. Chem. Soc.* **2004**, *126*, 6599.
- [84] O. Schafer, K. Klinker, L. Braun, D. Huesmann, J. Schultze, K. Koynov, M. Barz, *ACS Macro Lett.* **2017**, *6*, 1140.
- [85] S. Beck, J. Schultze, H. J. Rader, R. Holm, M. Schinnerer, M. Barz, K. Koynov, R. Zentel, *Polymers* **2018**, *10*, 141.
- [86] R. Roder, T. Preiss, P. Hirschele, B. Steinborn, A. Zimpel, M. Hohn, J. O. Radler, T. Bein, E. Wagner, S. Wuttke, U. Lachelt, *J. Am. Chem. Soc.* **2017**, *139*, 2359.
- [87] P. Schwille, F. J. MeyerAlmes, R. Rigler, *Biophys. J.* **1997**, *72*, 1878.
- [88] D. Schaeffel, R. H. Staff, H. J. Butt, K. Landfester, D. Crespy, K. Koynov, *Nano Lett.* **2012**, *12*, 6012.
- [89] M. A. Hood, U. Paiphansiri, D. Schaeffel, K. Koynov, M. Kappl, K. Landfester, R. Munoz-Espi, *Chem. Mater.* **2015**, *27*, 4311.
- [90] A. Huppertsberg, L. Kaps, Z. F. Zhong, S. Schmitt, J. Stickdorn, K. Deswarte, F. Combes, C. Czysch, J. De Vrieze, S. Kasmi, N. Choteschovsky, A. Klefenz, C. Medina-Montano, P. Winterwerber, C. J. Chen, M. Bros, S. Lienenklaus, N. N. Sanders, K. Koynov, D. Schuppan, B. N. Lambrecht, S. A. David, B. G. De Geest, L. Nuhn, *J. Am. Chem. Soc.* **2021**, *143*, 9872.
- [91] L. Nuhn, L. Braun, I. Overhoff, A. Kelsch, D. Schaeffel, K. Koynov, R. Zentel, *Macromol. Rapid Commun.* **2014**, *35*, 2057.
- [92] N. Leber, L. Kaps, M. Aslam, J. Schupp, A. Brose, D. Schaeffel, K. Fischer, M. Diken, D. Strand, K. Koynov, A. Tuetttenberg, L. Nuhn, R. Zentel, D. Schuppan, *Journal of Controlled Release* **2017**, *248*, 10.
- [93] K. Kristensen, J. R. Henriksen, T. L. Andresen, *Biochim. Biophys. Acta, Biomembr.* **2014**, *1838*, 2994.
- [94] G. R. Dakwar, E. Zagato, J. Delanghe, S. Hobel, A. Aigner, H. Denys, K. Braeckmans, W. Ceelen, S. C. De Smedt, K. Remaut, *Acta Biomater.* **2014**, *10*, 2965.
- [95] R. Bouchaala, L. Richert, N. Anton, T. F. Vandamme, S. Djabi, Y. Mely, A. S. Klymchenko, *ACS Omega* **2018**, *3*, 14333.
- [96] J. J. Mittag, B. Kneidl, T. Preibeta, M. Hossann, G. Winter, S. Wuttke, H. Engelke, J. O. Radler, *Eur. J. Pharm. Biopharm.* **2017**, *119*, 215.
- [97] M. Martinez-Negro, G. Gonzalez-Rubio, E. Aicart, K. Landfester, A. Guerrero-Martinez, E. Junquera, *Adv. Colloid Interface Sci.* **2021**, *289*, 102366.
- [98] T. Cedervall, I. Lynch, S. Lindman, T. Berggard, E. Thulin, H. Nilsson, K. A. Dawson, S. Linse, *Proc. Natl. Acad. Sci. USA* **2007**, *104*, 2050.
- [99] I. Alberg, S. Kramer, M. Schinnerer, Q. Z. Hu, C. Seidl, C. Leps, N. Drude, D. Moeckel, C. Rijcken, T. Lammers, M. Diken, M. Maskos, S. Morsbach, K. Landfester, S. Tenzer, M. Barz, R. Zentel, *Small* **2020**, *16*, 1907574.
- [100] S. Morsbach, G. Gonella, V. Mailander, S. Wegner, S. Wu, T. Weidner, R. Berger, K. Koynov, D. Vollmer, N. Encinas, S. L. Kuan, T. Bereau, K. Kremer, T. Weil, M. Bonn, H. J. Butt, K. Landfester, *Angew. Chem., Int. Ed.* **2018**, *57*, 12626.
- [101] C. Rocker, M. Potzl, F. Zhang, W. J. Parak, G. U. Nienhaus, *Nat. Nanotechnol.* **2009**, *4*, 577.

- [102] X. Jiang, S. Weise, M. Hafner, C. Rucker, F. Zhang, W. J. Parak, G. U. Nienhaus, *J. R. Soc., Interface* **2010**, *7*, S5.
- [103] P. Maffre, K. Nienhaus, F. Amin, W. J. Parak, G. U. Nienhaus, *Beilstein J. Nanotechnol.* **2011**, *2*, 374.
- [104] P. Maffre, S. Brandholt, K. Nienhaus, L. Shang, W. J. Parak, G. U. Nienhaus, *Beilstein J. Nanotechnol.* **2014**, *5*, 2036.
- [105] B. Pelaz, P. del Pino, P. Maffre, R. Hartmann, M. Gallego, S. Rivera-Fernández, J. M. de la Fuente, U. Nienhaus, W. J. Parak, *ACS Nano* **2015**, *9*, 6996.
- [106] Y. Klapper, P. Maffre, L. Shang, K. N. Ekdahl, B. Nilsson, S. Hettler, M. Dries, D. Gerthsen, G. U. Nienhaus, *Nanoscale* **2015**, *7*, 9980.
- [107] S. Alam, A. Mukhopadhyay, *J. Phys. Chem. C* **2014**, *118*, 27459.
- [108] I. Kohli, S. Alam, B. Patel, A. Mukhopadhyay, *Appl. Phys. Lett.* **2013**, *102*, 203705.
- [109] H. X. Wang, L. Shang, P. Maffre, S. Hohmann, F. Kirschhofer, G. Brenner-Weiss, G. U. Nienhaus, *Small* **2016**, *12*, 5836.
- [110] S. Milani, F. B. Bombelli, A. S. Pitek, K. A. Dawson, J. Radler, *ACS Nano* **2012**, *6*, 2532.
- [111] C. Czeslik, R. Jansen, M. Ballauff, A. Wittemann, C. A. Royer, E. Gratton, T. Hazlett, *Phys. Rev. E* **2004**, *69*, 021401.
- [112] S. Winzen, K. Koynov, K. Landfester, K. Mohr, *Colloids Surf., B* **2016**, *147*, 124.
- [113] O. Vilanova, J. J. Mittag, P. M. Kelly, S. Milani, K. A. Dawson, J. O. Radler, G. Franzese, *ACS Nano* **2016**, *10*, 10842.
- [114] M. Naito, T. Ishii, A. Matsumoto, K. Miyata, Y. Miyahara, K. Kataoka, *Angew. Chem., Int. Ed. Engl.* **2012**, *51*, 10751.
- [115] Y. Tsvetkova, N. Beztsinna, M. Baues, D. Klein, A. Rix, S. K. Golombek, W. Al Rawashdeh, F. Gremse, M. Barz, K. Koynov, S. Banala, W. Lederle, T. Lammers, F. Kiessling, *Nano Lett.* **2017**, *17*, 4665.
- [116] R. Holm, M. Douverne, B. Weber, T. Bauer, A. Best, P. Ahlers, K. Koynov, P. Besenius, M. Barz, *Biomacromolecules* **2019**, *20*, 375.
- [117] M. Darguzyte, R. Holm, J. Baier, N. Drude, J. Schultze, K. Koynov, D. Schwierz, S. M. Dadfar, T. Lammers, M. Barz, F. Kiessling, *Bioconjugate Chem.* **2020**, *31*, 2691.
- [118] R. Krzysztan, B. Salem, D. J. Lee, G. Schwake, E. Wagner, J. O. Radler, *Nanoscale* **2017**, *9*, 7442.
- [119] S. Pereira, R. S. Santos, L. Moreira, N. Guimaraes, M. Gomes, H. Zhang, K. Remaut, K. Braeckmans, S. De Smedt, N. F. Azevedo, *Pharmaceutics* **2021**, *13*, 989.
- [120] D. Van Lysebetten, A. Malfanti, K. Deswarte, K. Koynov, B. Golba, T. T. Ye, Z. F. Zhong, S. Kasmi, A. Lamoot, Y. Chen, S. Van Herck, B. N. Lambrecht, N. N. Sanders, S. Lienenklaus, S. A. David, M. J. Vicent, S. De Koker, B. G. De Geest, *ACS Appl. Mater. Interfaces* **2021**, *13*, 6011.
- [121] Y. Chen, G. R. Dakwar, K. Braeckmans, T. Lammers, W. E. Hennink, J. M. Metselaar, *Macromol. Biosci.* **2018**, *18*, 1700127.
- [122] S. Watanabe, K. Hayashi, K. Toh, H. J. Kim, X. Liu, H. Chaya, S. Fukushima, K. Katsushima, Y. Kondo, S. Uchida, S. Ogura, T. Nomoto, H. Takemoto, H. Cabral, H. Kinoh, H. Y. Tanaka, M. R. Kano, Y. Matsumoto, H. Fukuhara, S. Uchida, M. Nangaku, K. Osada, N. Nishiyama, K. Miyata, K. Kataoka, *Nat. Commun.* **2019**, *10*, 1894.
- [123] A. Tiiman, V. Jelic, J. Jarvet, P. Jaremo, N. Bogdanovic, R. Rigler, L. Terenius, A. Graslund, V. Vukojevic, *J. Alzheimer's Dis.* **2019**, *68*, 571.
- [124] S. Schmitt, A. Huppertsberg, A. Klefenz, L. Kaps, V. Mailänder, D. Schuppan, H.-J. Butt, L. Nuhn, K. Koynov, *Biomacromolecules* **2022**, <https://doi.org/10.1021/acs.biomac.1c01407>.
- [125] S. Wennmalm, P. Thyberg, L. Xu, J. Widengren, *Anal. Chem.* **2009**, *81*, 9209.
- [126] X. Fu, P. Sompol, J. A. Brandon, C. M. Norris, T. Wilkop, L. A. Johnson, C. I. Richards, *Nano Lett.* **2020**, *20*, 6135.
- [127] P. Schwille, U. Haupts, S. Maiti, W. W. Webb, *Biophys. J.* **1999**, *77*, 2251.
- [128] R. Rigler, *Biochem. Biophys. Res. Commun.* **2010**, *396*, 170.
- [129] R. A. Murray, Y. Qiu, F. Chiodo, M. Marradi, S. Penades, S. E. Moya, *Small* **2014**, *10*, 2602.
- [130] A. Silvestri, D. Di Silvio, I. Llarena, R. A. Murray, M. Marelli, L. Lay, L. Polito, S. E. Moya, *Nanoscale* **2017**, *9*, 14730.
- [131] E. L. Elson, *Traffic* **2001**, *2*, 789.
- [132] M. Wachsmuth, W. Waldeck, J. Langowski, *J. Mol. Biol.* **2000**, *298*, 677.
- [133] N. Malchus, M. Weiss, *J. Fluoresc.* **2010**, *20*, 19.
- [134] A. Pramanik, *Curr. Pharm. Biotechnol.* **2004**, *5*, 205.
- [135] K. Bacia, P. Schwille, *Methods* **2003**, *29*, 74.
- [136] P. Schwille, *Cell Biochem. Biophys.* **2001**, *34*, 383.
- [137] D. R. Larson, D. Zenklusen, B. Wu, J. A. Chao, R. H. Singer, *Science* **2011**, *332*, 475.
- [138] T. Ohrt, J. Muetze, W. Staroske, L. Weinmann, J. Hock, K. Crell, G. Meister, P. Schwille, *Nucleic Acids Res.* **2008**, *36*, 6439.
- [139] H. Glauner, I. R. Ruttekolk, K. Hansen, B. Steemers, Y. D. Chung, F. Becker, S. Hannus, R. Brock, *Br. J. Pharmacol.* **2010**, *160*, 958.
- [140] I. R. Ruttekolk, J. J. Witsenburg, H. Glauner, P. H. M. Bovee-Geurts, E. S. Ferro, W. P. R. Verdurmen, R. Brock, *Mol. Pharm.* **2012**, *9*, 1077.
- [141] R. Rezgui, K. Blumer, G. Yeoh-Tan, A. J. Trexler, M. Magzoub, *Biochim. Biophys. Acta, Biomembr.* **2016**, *1858*, 1499.
- [142] A. S. Klymchenko, E. Roger, N. Anton, H. Anton, I. Shulov, J. Vermot, Y. Mely, T. F. Vandamme, *RSC Adv.* **2012**, *2*, 11876.
- [143] A. Michelman-Ribeiro, D. Mazza, T. Rosales, T. J. Stasevich, H. Boukari, V. Rishi, C. Vinson, J. R. Knutson, J. G. McNally, *Biophys. J.* **2009**, *97*, 337.
- [144] K. M. Berland, P. T. C. So, E. Gratton, *Biophys. J.* **1995**, *68*, 694.
- [145] J. C. Politz, E. S. Browne, D. E. Wolf, T. Pederson, *Proc. Natl. Acad. Sci. USA* **1998**, *95*, 6043.
- [146] R. Brock, M. A. Hink, T. M. Jovin, *Biophys. J.* **1998**, *75*, 2547.
- [147] K. Bacia, S. A. Kim, P. Schwille, *Nat. Methods* **2006**, *3*, 83.
- [148] D. Di Silvio, M. Martinez-Moro, C. Salvador, M. D. Ramirez, P. R. Caceres-Velez, M. G. Ortore, D. Dupin, P. Andreatto, S. E. Moya, *J. Colloid Interface Sci.* **2019**, *557*, 757.
- [149] K. Remaut, B. Lucas, K. Raemdonck, K. Braeckmans, J. Demeester, S. C. De Smedt, *J. Controlled Release* **2007**, *121*, 49.
- [150] B. Lucas, K. Remaut, N. N. Sanders, K. Braeckmans, S. C. De Smedt, J. Demeester, *J. Controlled Release* **2005**, *103*, 435.
- [151] B. Lucas, K. Remaut, N. N. Sanders, K. Braeckmans, S. C. De Smedt, J. Demeester, *Biochemistry* **2005**, *44*, 9905.
- [152] S. Berezna, S. Schaefer, R. Heintzmann, M. Jahnz, G. Boese, A. Deniz, P. Schwille, *Biochim. Biophys. Acta* **2005**, *1669*, 193.
- [153] K. Remaut, B. Lucas, K. Braeckmans, N. N. Sanders, J. Demeester, S. C. De Smedt, *J. Controlled Release* **2005**, *110*, 212.
- [154] S. Draffehn, M. U. Kümke, *Mol. Pharm.* **2016**, *13*, 1608.
- [155] T. Fritz, M. Voigt, M. Worm, I. Negwer, S. S. Müller, K. Kettenbach, T. L. Ross, F. Roesch, K. Koynov, H. Frey, M. Helm, *Chem. - Eur. J.* **2016**, *2231*, 11578.
- [156] R. Bouchaala, N. Anton, H. Anton, T. Vandamme, J. Vermot, D. Smail, Y. Mely, A. S. Klymchenko, *Colloids Surf., B* **2017**, *156*, 414.
- [157] K. Eisele, R. A. Gropeanu, C. M. Zehendorf, A. Rouhanipour, A. Ramanathan, G. Mihov, K. Koynov, C. R. Kuhlmann, S. G. Vasudevan, H. J. Luhmann, T. Weil, *Biomaterials* **2010**, *31*, 8789.
- [158] S. L. Kuan, B. Stockle, J. Reichenwallner, D. Y. Ng, Y. Wu, M. Doroshenko, K. Koynov, D. Hinderberger, K. Mullen, T. Weil, *Biomacromolecules* **2013**, *14*, 367.
- [159] S. L. Kuan, D. Y. Ng, Y. Wu, C. Fortsch, H. Barth, M. Doroshenko, K. Koynov, C. Meier, T. Weil, *J. Am. Chem. Soc.* **2013**, *135*, 17254.
- [160] R. Lizatovic, M. Assent, A. Barendregt, J. Dahlin, A. Bille, K. Satzinger, D. Tupina, A. J. R. Heck, S. Wennmalm, I. Andre, *Angew. Chem., Int. Ed. Engl.* **2018**, *57*, 11334.
- [161] S. Wuttke, S. Braig, T. Preiss, A. Zimpel, J. Sicklinger, C. Bellomo, J. O. Radler, A. M. Vollmar, T. Bein, *Chem. Commun.* **2015**, *51*, 15752.
- [162] T. Preiss, A. Zimpel, S. Wuttke, J. O. Radler, *Materials* **2017**, *10*, 216.

- [163] T. T. Morgan, H. S. Muddana, E. I. Altinoglu, S. M. Rouse, A. Tabakovic, T. Tabouillot, T. J. Russin, S. S. Shanmugavelandy, P. J. Butler, P. C. Eklund, J. K. Yun, M. Kester, J. H. Adair, *Nano Lett.* **2008**, *8*, 4108.
- [164] H. S. Muddana, T. T. Morgan, J. H. Adair, P. J. Butler, *Nano Lett.* **2009**, *9*, 1559.
- [165] K. Ma, U. Werner-Zwanziger, J. Zwanziger, U. Wiesner, *Chem. Mater.* **2013**, *25*, 677.
- [166] K. Ma, D. H. Zhang, Y. Cong, U. Wiesner, *Chem. Mater.* **2016**, *28*, 1537.
- [167] A. Kienzle, S. Kurch, J. Schloder, C. Berges, R. Ose, J. Schupp, A. Tuettenberg, H. Weiss, J. Schultze, S. Winzen, M. Schinnerer, K. Koynov, M. Mezger, N. K. Haass, W. Tremel, H. Jonuleit, *Adv. Healthcare Mater.* **2017**, *6*, 1700012.
- [168] Y. Yi, H. J. Kim, P. Mi, M. Zheng, H. Takemoto, K. Toh, B. S. Kim, K. Hayashi, M. Naito, Y. Matsumoto, K. Miyata, K. Kataoka, *J. Controlled Release* **2016**, *244*, 247.
- [169] D. V. Kolygina, M. Siek, M. Borkowska, G. Ahumada, P. Barski, D. Witt, A. Y. Jee, H. Miao, J. C. Ahumada, S. Granick, K. Kandere-Grzybowska, B. A. Grzybowski, *ACS Nano* **2021**, *15*, 11470.
- [170] L. W. Shao, C. Q. Dong, F. M. Sang, H. F. Qian, J. C. Ren, *J. Fluoresc.* **2009**, *19*, 151.
- [171] Y. Z. Wu, K. Eisele, M. Doroshenko, G. Algara-Siller, U. Kaiser, K. Koynov, T. Weil, *Small* **2012**, *8*, 3465.
- [172] C. Q. Dong, J. Irudayaraj, *J. Phys. Chem. B* **2012**, *116*, 12125.
- [173] R. L. Liu, D. Q. Wu, S. H. Liu, K. Koynov, W. Knoll, Q. Li, *Angew. Chem., Int. Ed.* **2009**, *48*, 4598.
- [174] Q. Li, T. Y. Ohulchanskyy, R. L. Liu, K. Koynov, D. Q. Wu, A. Best, R. Kumar, A. Bonoiu, P. N. Prasad, *J. Phys. Chem. C* **2010**, *114*, 12062.
- [175] M. Righetto, A. Privitera, I. Fortunati, D. Mosconi, M. Zerbetto, M. L. Curri, M. Corricelli, A. Moretto, S. Agnoli, L. Franco, R. Bozio, C. Ferrante, *J. Phys. Chem. Lett.* **2017**, *8*, 2236.
- [176] F. Neugart, A. Zappe, F. Jelezko, C. Tietz, J. P. Boudou, A. Krueger, J. Wrachtrup, *Nano Lett.* **2007**, *7*, 3588.
- [177] Y. Y. Hui, B. L. Zhang, Y. C. Chang, C. C. Chang, H. C. Chang, J. H. Hsu, K. Chang, F. H. Chang, *Opt. Express* **2010**, *18*, 5896.
- [178] D. A. Simpson, A. J. Thompson, M. Kowarsky, N. F. Zeeshan, M. S. J. Barson, L. T. Hall, Y. Yan, S. Kaufmann, B. C. Johnson, T. Ohshima, F. Caruso, R. E. Scholten, R. B. Saint, M. J. Murray, L. C. L. Hollenberg, *Biomed. Opt. Express* **2014**, *5*, 1250.
- [179] W. N. Liu, B. Naydenov, S. Chakraborty, B. Wuensch, K. Hubner, S. Ritz, H. Colfen, H. Barth, K. Koynov, H. Y. Qi, R. Leiter, R. Reuter, J. Wrachtrup, F. Boldt, J. Scheuer, U. Kaiser, M. Sison, T. Lasser, P. Tinnefeld, F. Jelezko, P. Walther, Y. Z. Wu, T. Weil, *Nano Lett.* **2016**, *16*, 6236.

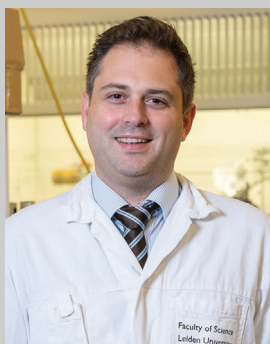


**Sascha Schmitt** obtained his M.Sc. degree in chemistry at the Johannes-Gutenberg University Mainz, Germany. Currently, he is undertaking a Ph.D. at the Max Planck Institute for Polymer Research in Mainz, Germany, in the group of Prof. Butt. His research focuses on nanocarrier characterization in different environments reaching from buffer to full blood using the fluorescence correlation spectroscopy and time correlated single photon counting techniques.



**Lutz Nuhn** studied biomedical chemistry and obtained his Ph.D. in the group of Rudolf Zentel at the Johannes Gutenberg-University Mainz (Germany) in 2014. After a postdoctoral research stay with Bruno De Geest at Ghent University (Belgium), he became group leader at the Max Planck Institute for Polymer Research (MPI-P) with Tanja Weil. Lutz Nuhn received scholarships from the German National Academic Foundation, the Max Planck Graduate School, the Alexander-von-Humboldt-Foundation, the Research Foundation Flanders, the Fonds der Chemischen Industrie and the Max-Buchner-Foundation. Since 2019, he has been appointed Emmy Noether group leader of the Macromolecular Therapeutics Lab at the MPI-P.





**Matthias Barz** studied chemistry at the Johannes Gutenberg-University (JGU) (Mainz, Germany) and Seoul National University (South Korea) received a Ph.D. in polymer chemistry from the JGU in 2010. Before starting his independent research, he worked in the laboratories of Maria J. Vicent (Valencia, Spain) and Tom Kirchhausen (Boston Children's Hospital, USA). Since 2020 he is full professor at the Leiden Academic Center for Drug Research (LACDR) at Leiden University (Netherlands). His research focuses on the development of polypept(o)ides, polymers combining polypeptides with polypeptoids, for the synthesis of functional nanoparticles for cancer immune therapy, cancer theranostics, and antibacterial therapies.



**Hans-Jürgen Butt** studied physics in Hamburg and Göttingen. He did his Ph.D. at the Max Planck Institute for Biophysics, Frankfurt, in 1989. After a postdoc in Santa Barbara and a researcher position back in Frankfurt, he became associate professor at the University Mainz and three years later full professor at the University of Siegen. In 2002 he joined the Max Planck Institute for Polymer Research in Mainz as a director. His research is on the structure and dynamics of soft matter interfaces including wetting and surfaces forces using methods such as scanning probe microscopy, fluorescence correlation spectroscopy, and X-ray scattering.



**Kaloian Koynov** studied physics and obtained his Ph.D. at the Sofia University, Bulgaria in 1997. After a postdoctoral stay in the University Paris Sud, France in 2000 he joined the department of Wolfgang Knöll at the Max Planck Institute for Polymer Research in Mainz, Germany as a postdoc and EU Marie Curie Fellow. Since 2006 he is a group leader in the department of Hans-Jürgen Butt at the Max Planck Institute for Polymer Research. His research is focused on the development and application of fluorescence correlation spectroscopy as a versatile tool in polymer, colloid, and interface science.